SAND75-0669
Unlimited Release

Instrumentation and Process Control Development for in Situ Coal Gasification

Fourth Quarterly Report: September through November 1975

David A. Northrop, Editor

Prepared by Sandia Laboratories, Albuquerque, New Mexico 87115 and Livermore, California 94550 for the United States Energy Research and Development Administration under Contract AT (29-1)-789
Printed January 1976

When printing a copy of any digitized SAND Report, you are required to update the markings to current standards.

Sandia Laboratories
energy report

SF 2900 QQB(3-74)

Issued by Sandia Laboratories, operated for the United States Energy Research and Development Administration by Sandia Corporation.

NOTICE

This report was prepared as an account of work sponsored by the United States Government. Neither the United States nor the United States Energy Research and Development Administration, nor any of their employees, nor any of their contractors, subcontractors, or their employees, makes any warranty, express or implied, or assumes any legal liability or responsibility for the accuracy, completeness or usefulness of any information, apparatus, product or process disclosed, or represents that its use would not infringe privately owned rights.

Printed in the United States of America
Available from:
National Technical Information Service
U. S. Department of Commerce
5285 Port Royal Road
Springfield, VA 22151
Price: Printed Copy $5.00; Microfiche $2.25

* Add $2.50 per copy for foreign price.

SAND-75-0669
Unlimited Release

INSTRUMENTATION AND PROCESS CONTROL DEVELOPMENT FOR IN SITU COAL GASIFICATION

Fourth Quarterly Report: September through November 1975

Edited by: David A. Northrop, Supervisor
Underground Process Control Division
Sandia Laboratories
Albuquerque, New Mexico 87115

HIGHLIGHTS

Field Instrumentation

The instrumentation effort for Phases 2 and 3 of the Second Hanna In Situ Coal Gasification Experiment was fielded and background data obtained prior to the initiation of Phase 2 on November 25, 1975. A total of over 600 channels of instrumentation in 15 instrumentation wells and two surface arrays was fielded for the different instrumentation techniques under evaluation (p. 8).

Instrumentation Analysis

Acoustic: The feasibility of the passive acoustic technique to locate the source of process-related noises has been demonstrated. The utility of this technique is presently hampered by the inexact definition of signal arrivals and the lack of automated signal monitoring and analysis systems (p. 20).

Electrical: A revised mathematical model for the electrical techniques has been developed which demonstrates the potential of these techniques for remote monitoring (p. 27). These calculations have been used in the interpretation of the limited Phase 1 data (p. 31).

Intentionally Left Blank

TABLE OF CONTENTS

		Page
I.	INTRODUCTION	7
II.	FIELDING SUMMARY, PHASES 2 AND 3 (J. A. Beyeler, 1123, and W. C. Wilson, 1133)	8
III.	INSTRUMENTATION SUMMARY, PHASES 2 AND 3 (D. A. Northrop, 5732)	12
IV.	TEMPERATURE	17
	A. In Situ Temperature Measurements (S. G. Beard, 5732, and R. P. Reed, 1116)	17
	B. Thermal Instrumentation (R. P. Reed, 1116)	20
V.	SEISMIC-ACOUSTIC STUDIES	20
	A. Assessment of Passive Acoustic Techniques (L. W. Beckham, 5732)	20
	B. Induced Seismic Experiments, Phases 2 and 3 (L. W. Beckham, 5732, and H. D. Garbin, 1111)	23
	C. Refraction Calculations (H. D. Garbin, 1111)	25
	D. Simulation Studies (A. G. Beattie, J. C. Bushnell, and J. H. Gieske, all 9352)	25
	E. Hardware Development for Data Collection and Transmission (T. M. Schultheis, 9423, and L. W. Beckham, 5732)	27
VI.	ELECTRICAL STUDIES	27
	A. Mathematical Modeling of the Electrical Measurements (L. C. Bartel, 5732)	27
	B. Interpretation of Phase 1 Electrical Resistivity Data (L. C. Bartel, 5732, and R. W. Seavey, 5733)	31
	C. Electrical Instrumentation, Phases 2 and 3 (R. W. Seavey, 5733, and L. C. Bartel, 5732)	34
VII.	SUPPORTING STUDIES	35
	A. Grout Properties and Behavior (S. G. Beard, 5732, Coordinator)	35
	B. Thermal Conductivity of Core Samples (R. U. Acton, 5842)	35
	C. Specific Heat of Hanna Coal (H. P. Stephens, 5842)	36
	D. Systems Studies (R. E. D. Stewart and J. A. Allensworth, 5742)	37
VIII.	PUBLICATIONS, PRESENTATIONS, AND BRIEFINGS	41

LIST OF TABLES

I.	Downhole Instrumentation Locations; Phases 2 and 3	14
II.	Instrumentation Techniques to be Fielded and Evaluated on the Second Hanna In Situ Coal Gasification Experiment	17

LIST OF TABLES (Contd.)

III. Vertical Placement of Temperature Sensing Points Relative to Instrument Reference at Installation 21

IV. Thermal Conductivity of Grout: Preliminary Data 36

V. Specific Heat of Hanna Coal 37

VI. Brayton Cycle Efficiencies for Various System Configurations, Fuel Inlet Conditions, Turbine Inlet Temperatures and Compression Ratios 38

VII. Effect of Fuel Heating Value (H) on Combustion Temperature (T), Net Turbine Output (W), and Cycle Efficiency (η) for a Simple Brayton Cycle with Pressure Ratio = 16 and Fuel Supplied @ 100°F and 1 ATM 39

VIII. Rankine Cycle Efficiencies for System Utilizing Multiple Feedwater Heaters and Either "Hot" or "Cold" Fuel Gas Cleanup 41

LIST OF ILLUSTRATIONS

Fig. 1. Well Locations for Phases 2 and 3 of the Hanna II Experiment (November 1975) 9

Fig. 2. Phase 2 and 3 Site After Fielding; November 1975. View to Northwest; Well 7 in Foreground. 11

Fig. 3. Phase 2 and 3 Site After Fielding; November 1975. View to the South from Well S1; Well A in Foreground 11

Fig. 4. Instrumentation and Well Layout for Phases 2 and 3 of the Hanna II Underground Coal Gasification Experiment 13

Fig. 5. Selected Temperatures in Well AA During Phase 1b and Quench 18

Fig. 6. Selected Temperatures in Well BB During Phase 1b and Quench 18

Fig. 7. Temperatures in Well AA Immediately Before and During Water Injection 19

Fig. 8. Frequency of Type A Signals During Phase 1 (Number per five-minute interval received in enough channels to allow tri-angulation) 22

Fig. 9. Source Locations for Selected Discrete Signals Recorded During Days 168 and 171, Phase 1a. 24

Fig. 10. Normalized Transmission Coefficient for Different Frequencies as a Function of Incident Angle 26

Fig. 11. Schematic Layout for the Model Calculations 28

Fig. 12. $|E_x|/I$ versus x Measured at the Surface with No Instrumentation Wells Present 29

Fig. 13. $|E_x|/I$ versus x Measured at the Surface with Two Instrumentation Wells Present 29

Fig. 14. $|\Delta\phi|/I$ at Midseam as Measured Between Wells M and N as a Function of "Time" for the Carbonized Path Locations Shown in the Insert 30

Fig. 15. Observed Resistivity for Selected Surface Gauge Locations During Phase 1 32

Fig. 16. Plot of Surface Resistivities Measured on Day 158, Phase 1 33

Fig. 17. Rankine Power Cycle System with Two Feedwater Heaters 40

I. INTRODUCTION

This is the fourth quarterly report for Sandia Laboratories' program on Instrumentation and Process Control Development for In Situ Combustion Recovery Processes.* This report summarizes program activities in conjunction with the Laramie Energy Research Center's (LERC) underground coal gasification program and experiments at Hanna, Wyoming between September 1, 1975, and November 30, 1975. The Second Hanna Experiment is currently underway. Phase 1 was fielded and conducted between January and August 1975; construction and fielding for Phases 2 and 3 and initiation of Phase 2 were completed by the end of this quarter.

Sandia program activities have occurred in several areas during the past quarter:

1. The instrumentation effort for Phases 2 and 3 was fielded. This effort included fifteen instrumentation wells, two shot wells for the induced seismic studies, and surface resistivity probe and geophone arrays. A total of twelve different instrumentation techniques will be exercised.

2. Background data for the unperturbed site were obtained for the electrical resistivity and induced seismic experiments prior to the initiation of Phase 2 in late November.

3. Analytical efforts were continued for each of the instrumentation techniques to aid in data reduction, interpretation, correlation and modeling of the field experiment. The feasibility of the passive acoustic technique was demonstrated. Improved modeling calculations have been made which show the potential of the electrical methods for remote detection. Revised data reduction and communication procedures for all techniques for Phases 2 and 3 have been formulated.

4. Work has been initiated on the development of second generation instrumentation systems for future field programs. These will feature on-site, real-time data acquisition, analysis, and display systems. An overall computer-based systems definition is under study and hardware development for specific subsystems has been initiated.

5. Studies have continued in the areas of material properties and systems analysis. Particular emphasis is being placed upon grout properties and behavior during gasification as they affect the downhole instrumentation.

---

* First Quarterly Report, December 1974 through February 1975, Sandia Laboratories Report, SAND-75-0200, April 1975.

Second Quarterly Report, March through May 1975, Sandia Laboratories Report, SAND-75-0366, June 1975.

Third Quarterly Report, June through August 1975, Sandia Laboratories Report, SAND-75-0535, October 1975.

Activities which can be expected during the next quarter (through February 1976) include:

1. The field experiment will be monitored. Present schedules show the following events to occur: combustion linkage and quenching between Wells 7 and 8 (Phase 2a); air injection, ignition, combustion and gasification between Wells 5 and 6 (Phase 2b); and, possibly, air injection into Wells 7 and 8 to initiate Phase 3.

2. All instrumentation techniques are expected to be exercised during the gasification between Wells 5 and 6. Timely analyses of field data as they become available will be emphasized.

3. Analysis and modeling of Phase 1 results and in other areas will continue. Reports now in preparation are expected in the areas of passive acoustics, electrical modeling, thermal history of Phase 1, and systems analysis.

4. Activities in the areas of material properties, laboratory support, on-site data systems development, and systems analysis will continue.

II. FIELDING SUMMARY, PHASES 2 AND 3

(J. A. Beyeler, 1123 and W. C. Wilson, 1133)

The fielding plans for Phases 2 and 3 evolved from numerous discussions involving both Sandia and LERC personnel throughout the late spring and early summer. Phase 1 results were used extensively in the derivation of the plans and a revised instrumentation effort as presented in the Third Quarterly Report. A special joint meeting was held on July 16, 1975, at Hanna to finalize these plans and establish a coordinated fielding plan. The well locations are shown in Figure 1. LERC's drilling and coring of the four injection-production wells (Wells 5, 6, 7 and 8) began on July 21, whereas Sandia's fielding activities commenced on August 18 with the drilling of its first well. LERC's construction and installation of process-related systems and Sandia's instrumentation fielding were essentially completed by November 15, 1975.

The site for Phases 2 and 3 lies north and slightly west of the Phase 1 site. Relocation of five LERC buildings and two Sandia trailers to this new site was required. The Well 5-6 and 7-8 lines lie in the same direction, N60E, as the Well 1-3 line in Phase 1. The depth to the bottom of the coal seam remained at approximately 300 ft. Logs were obtained by Sandia on Wells S1 and S2 to depths of approximately 450 and 350 ft, respectively. These logs were used to confirm the geology encountered at the Phase 1 site, obtain sonic velocity, density and electrical resistivity geologic data, and to confirm the straightness and verticality of the wells. The same driller (J. Camp, Medco Inc., Ft. Collins, CO) was employed and the same excellent verticality and straightness were obtained as in Phase 1, thus eliminating the need for directional logs for each well. Visual inspection and hand-line and direction logs confirmed the verticality (within a foot at total depth) attainable by this driller and his heavy equipment. LERC cores obtained through the coal seam were

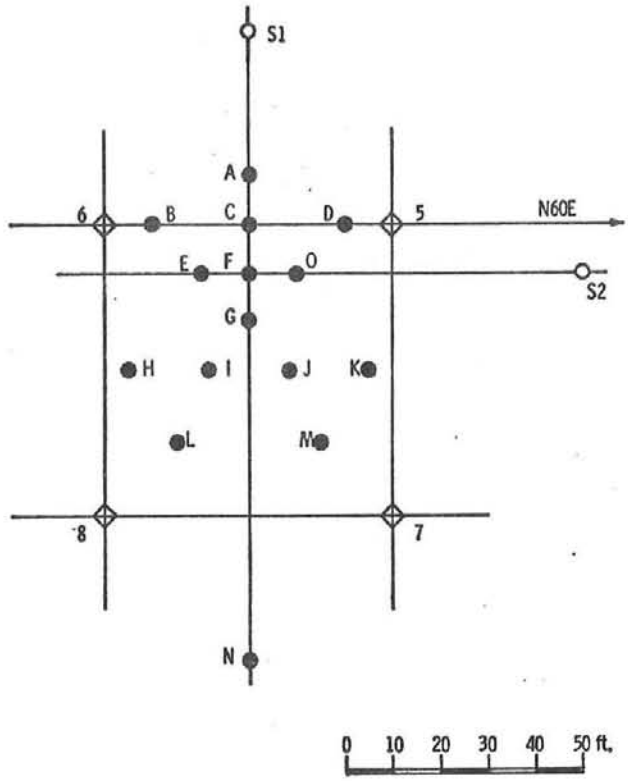

Figure 1. Well Locations for Phases 2 and 3 of the Hanna II Experiment (November 1975).

used to locate the bottom of the coal seam. This reference depth was then calculated for each of the instrument wells and used to locate the instrument strings.

Essentially the same fielding procedures (use of a messenger cable, measuring tape, the "chapel" trailer, etc.) were employed as described in the First Quarterly Report. A sequential drilling, fielding, and grouting operation was used; no more than three days (usually two) were required to complete any well. The overall fielding activity proceeded relatively smoothly due to the experience gained in Phase 1 and the fair weather conditions.

The sloughing problems encountered in Phase 1 continued unabated at this neighboring site. Plans were altered to include the use of casing to approximately 165-180 ft depth; this depth is below the sloughing zone and approximately 90-105 ft above the top of the coal seam. No further problems due to sloughing were encountered after this procedure was adopted. However, this procedure did require added expense for casing and driller's time and effort for drilling, reaming, and setting casing.

The grouting procedures were changed from those in Phase 1 and more reliability and less trouble was encountered. (Grout formulation and emplacement were again performed by Waterways Experiment Station, United States Corps of Engineers, Vicksburg,

MS.) The two-stage, coal-filled grout procedure was not used on the basis that its benefit did not out-weigh the problems that had been encountered during Phase 1. Two slightly different cement-fly ash grout mixtures were placed in each well in a continuous grouting operation. The plastic grout hoses could not be fully removed from Wells A and M as they apparently hung up on the smaller diameter casing used in these wells. However, a reliable grout column to the surface was believed to have been established in each case. In Well J, the instrument string had to be removed and reinstalled when it was discovered (before grouting) that the grout hose was blocked; subsequent completion was without incident.

Downhole installation was performed in two periods: two shot wells and eight instrumentation wells between August 18 and September 20, and seven instrumentation wells between October 6 and October 20. The latter date barely beat the first winter storm. The two week interim period was necessitated by the need to fabricate the remainder of the thermocouple strings, an activity which was more time consuming than anticipated. The installation of the surface resistivity probe and geophone array was also completed by the end of October. The balance of the time was taken by stringing of the sensor leads and cables to, and patching them within, the instrumentation trailer. As the total number of sensors and accessory circuits was well over 600, this was a time-consuming task. Intermediate patch panels were installed in all geophone, resistivity, and thermocouple circuits in order to increase the flexibility of collecting different measurements. Severe noise and ground loop problems were experienced during installation and systems checkout, but these have apparently been eliminated.

Overall, the new site and installation has an improved appearance over the Phase 1 site fielded last winter, and points out the visible benefits of fielding in clement weather. Instrumentation cables are contained in overhead cable trays from each well to the recording trailer and all surface probes and cables have been buried to provide free access to the site. Photos of the completed site are shown in Figures 2 and 3.

A special firing system was designed and built by Division 1132 to fire the strings of twelve detonators in Wells S1 and S2 for the induced seismic experiment. This firing system uses a digital clock to provide the time base for the programmable timing intervals (presently 5 sec) which trigger individual X-units (TC132) charged to 3 kv by a series-parallel arrangement of high voltage power supplies (TC369). A time reference fiducial accurate to ±1 μsec is furnished to the recording system when each X-unit fires its detonator. The system incorporates redundancy in its trigger circuits and charging networks and includes the standard safety features. The system is housed in a small shed constructed over the shot wells. Based on operational problems encountered during background seismic data collection, multicircuit detonator cables and winch assemblies are being fabricated.

Background or quiet time seismic and resistivity data were obtained in late November prior to the initiation of Phase 2. Air injection into Well 7 with production at Well 8 was initiated on November 25 (Julian Day 329). Ignition occurred on December 3 (Day 337). There are no instrumentation wells within 15 ft of the line

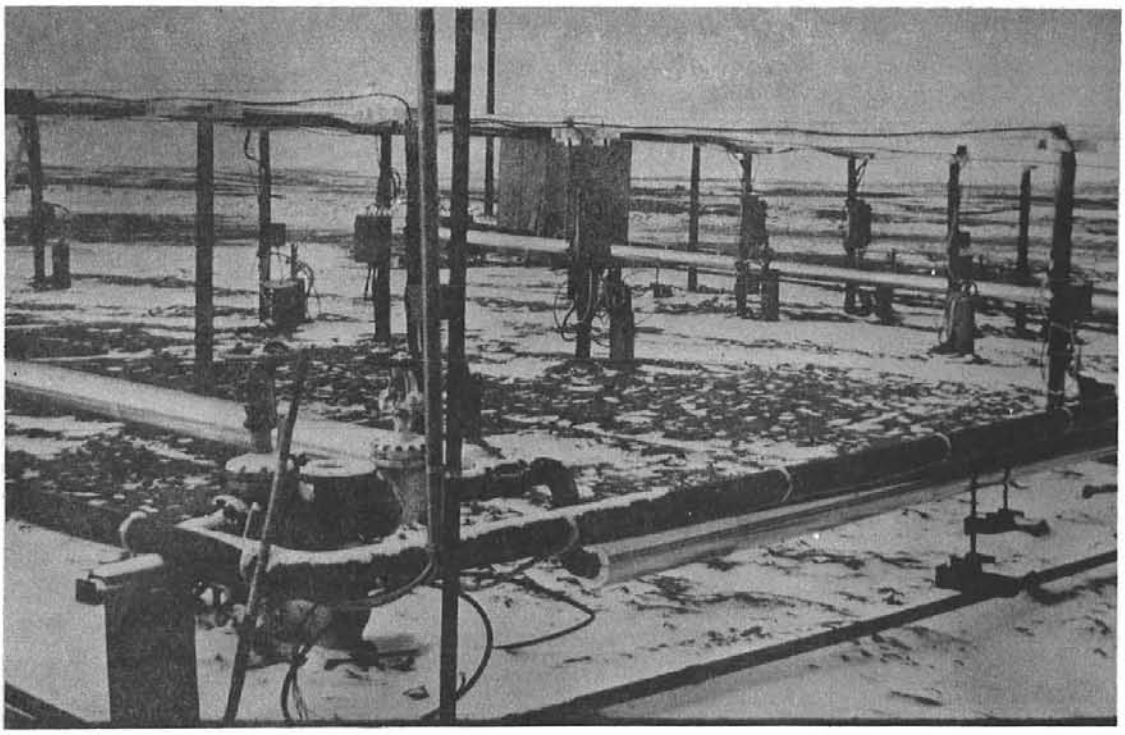

Figure 2. Phase 2 and 3 Site After Fielding; November 1975. View to the northwest; Well 7 in foreground.

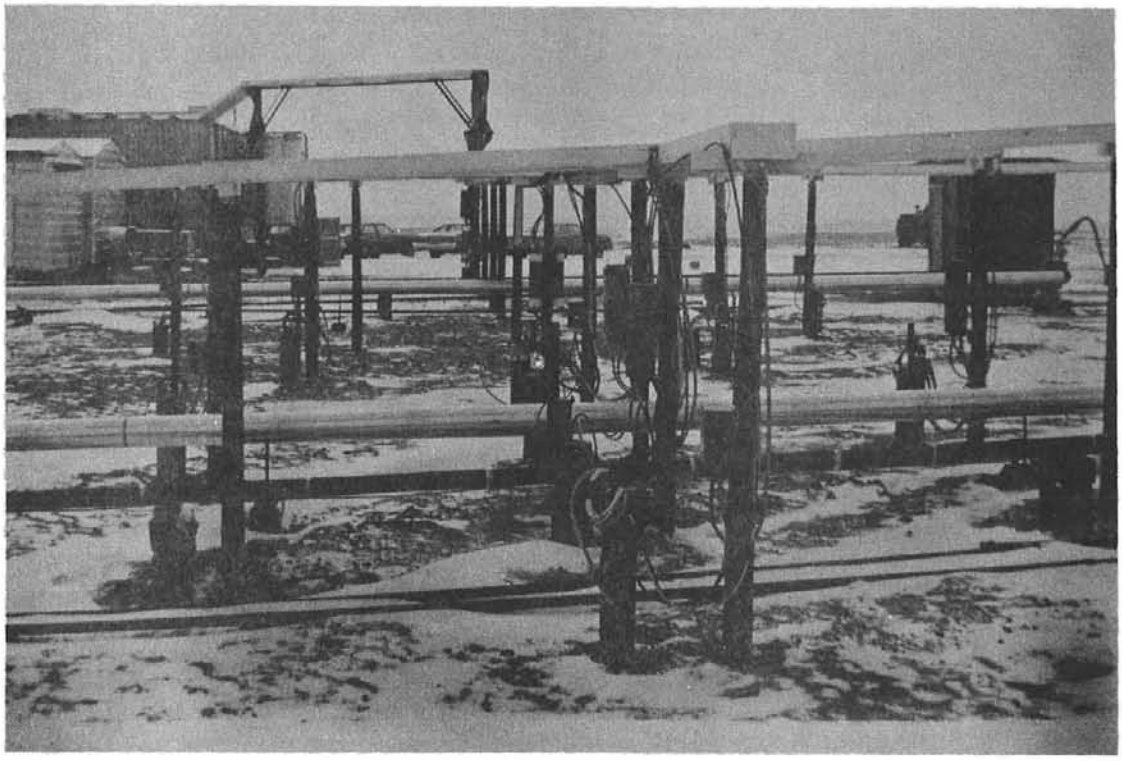

Figure 3. Phase 2 and 3 Site After Fielding; November 1975. View to the south from near Well S1; Well A in foreground.

between Wells 7 and 8 and based upon Phase 1 experience, thermal effects will not be detected during this combustion linking activity. However, induced seismic and resistivity data are being obtained at regular intervals.

III. INSTRUMENTATION SUMMARY, PHASES 2 AND 3 (D. A. Northrop, 5732)

A revised instrumentation concept for Phases 2 and 3 has been fielded. The revisions were based upon Phase 1 experience and reinterpretation of Hanna I results in light of Phase 1 data. Location of the fifteen instrumentation wells and the two shot wells for the induced seismic experiment is shown in Figure 1. This layout plus the surface resistivity probe and geophone arrays are shown in Figure 4. (Well and sensor locations for Phase 1, sometimes discussed in this report, are given as Figure 1 and Table I, respectively, in the Third Quarterly Report.)

The locations for all downhole instrumentation are summarized in Table I. All sensor locations are referenced to the coal seam floor-sandstone interface depth obtained from LERC cores taken on Wells 5, 6, 7 and 8 and from relative well collar and ground elevations. A measuring tape was fastened the entire length of the messenger cable to aid in location of the different sensors. Overall string position is determined by the calculated collar to reference depth; differences are due to formation dip and different collar elevations.

Salient features in this instrumentation concept for Phases 2 and 3 as fielded are summarized below. In most cases, further details are presented in the appropriate sections elsewhere in this report.

1. The new well pattern is designed to improve spatial resolution of Phase 2 and 3 events. Wells A, B, C, D, E, F and O are intended to provide a detailed spatial description of linkage and gasification between a pair of wells (Wells 5 and 6, Phase 2). Wells G, H, I, J, K, L and M are intended to provide an assessment of the uniformity of the line drive or areal sweep between Wells 5-6 and 7-8 (Phase 3).

2. Different configurations for the electrical measurements have been included. The surface and downhole resistivity probes will be driven both by using outlying surface current wells and by using Well 5. The latter provides a changing current electrode geometry in the form of coal carbonized during gasification. Outlying resistivity probes have been added to provide background data and changes related to surface conditions and telluric currents.

3. A fifteen geophone surface array has been emplaced at approximately 20 ft depth; it will be used for the evaluation of a downhole-to-surface induced seismic technique based upon signals induced below the coal seam in Well S1.

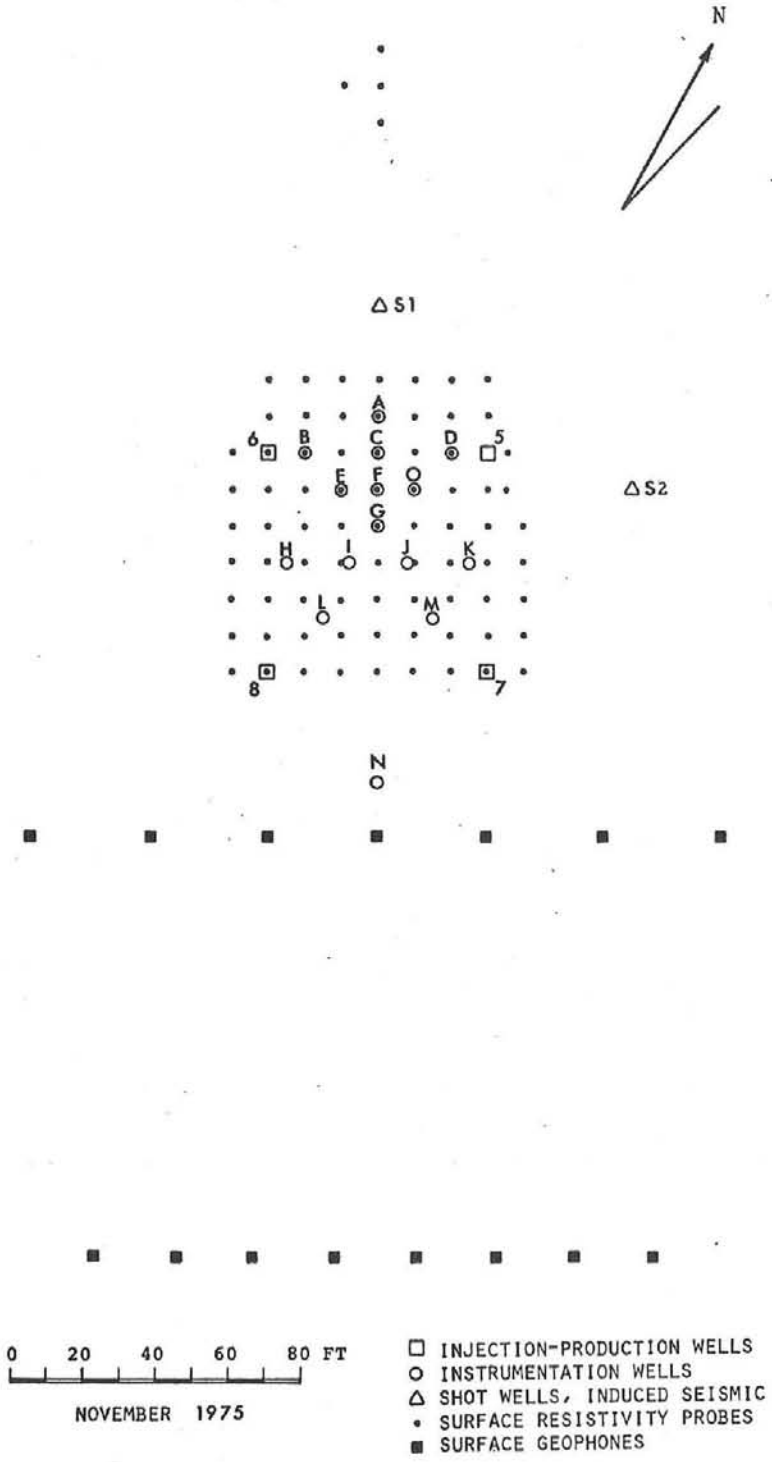

Figure 4. Instrumentation and Well Layout for Phases 2 and 3 of the Hanna II Underground Coal Gasification Experiment.

TABLE I - DOWNHOLE INSTRUMENTATION LOCATIONS; PHASES 2 AND 3

		WELL A	WELL B	WELL C	WELL D	WELL E	WELL F	WELL O	WELL G
Installation Date		10/18/75	10/15/75	10/8/75	9/20/75	10/20/75	10/17/75	10/10/75	10/16/75
Well Collar to Reference[1]		299.3 ft	297.1 ft	299.2 ft	301.7 ft	298.1 ft	299.7 ft	300.6 ft	299.2 ft
Geophones	a	60.0	60.0	60.0	60.0	60.0	60.0	60.0	120.0[5]
	b	50.0	50.0	50.0	50.0	50.0	50.0	50.0	105.0
	c	40.0[2]	40.0	40.0	40.0	40.0	40.0[2]	40.0	90.0
	d	30.0	30.0	30.0	30.0	30.0	30.0	30.0	75.0
	e	22.5	22.5	22.5	22.5	22.5	22.5	22.5	60.0
	f	15.0	15.0	15.0	15.0	15.0	15.0	15.0	45.0
	g	7.5	7.5	7.5	7.5	7.5	7.5	7.5	30.0
	h	0.0	0.0	0.0	0.0	0.0	0.0	0.0	15.0
	i	-10.0	-10.0	-10.0	-10.0	-10.0	-10.0	-10.0	0.0
	j	-20.0	-20.0	-20.0	-20.0	-20.0	-20.0	-20.0	-20.0
Resistivity Probes	a	32.0	31.7	32.0	32.1	32.1[4]	32.0[4]	32.0	32.0
	b	16.0	16.0	16.0	16.0	16.3[4]	16.1[4]	16.0	16.5
	c	-2.0	-3.0	-2.0	-2.0	-2.0[4]	-2.0[4]	-2.0	-2.0
Thermocouple Levels (Low Temp)	a	74.3	69.3	35.2	64.1	35.0	35.5	52.9	35.3
	b	49.0	35.1	32.7	30.2	30.3	30.3	35.2	30.6
	c	30.2	32.5	30.2	30.0	25.0	30.2	30.0	30.4
	d	30.0	30.0	25.1	20.2	20.2	25.2	25.0	25.3
	e	25.2	27.7	20.1[3]	15.1	20.1	20.2[3]	20.0	20.2
	f	22.5	22.6	14.9	12.7	15.0	15.5	14.9	15.6
	g	20.1	17.9	10.5	10.1	10.0	10.1	10.3	10.4
	h	17.6	15.2	5.0	7.7	5.1	5.1	5.0	5.3
	i	15.1	12.5	-0.1	5.2	0.0	0.0	0.0	0.0
	j	12.5	5.2	-	2.8	-	-	-	-
	k	10.0	0.2	-	0.2	-	-	-	-
	l	0.0	-2.4	-	-10.0	-	-	-	-
Thermocouple Levels (High Temp)	a	-	65.0	65.0	-	65.0	65.0	-	-
	b	-	20.0[3]	15.0[3]	-	20.0[3]	20.2[3]	-	-
	c	-	15.0	-	-	15.0[3]	16.0	-	-
	d	-	-	-	-	-	15.0	-	-
Gas Sampling Canister		-	19.0	19.0	19.0	19.0	19.0	19.0	19.0
Pressure Transducer		-	-	19.5	-	-	19.5	-	19.5
Tilt Meters	a	-	67.2	71.0	-	-	71.0	-	-
	b	-	55.0	55.0	-	-	55.0	-	-
Displacement Gauge	reference	-	-	107.3	-	104.9	-	-	104.9
	a	-	-	83.9	-	83.6	-	-	83.6
	b	-	-	62.5	-	62.4	-	-	62.3
	c	-	-	50.0	-	50.1	-	-	50.1
	d	-	-	35.0	-	35.0	-	-	35.0

NOTES:
(1) Locations are referenced to the bottom of the coal seam in each well. Positive and negative numbers are distances in feet above and below the reference, respectively.
(2) 10x downhole amplifier fielded.
(3) Two thermocouples at this level.
(4) High temperature resistivity probes and cables.
(5) 100x downhole amplifier fielded.

TABLE I (Continued)

		WELL H	WELL I	WELL J	WELL K	WELL L	WELL M	WELL N	WELL S1
Installation Date		9/18/75	9/16/75	9/11/75	9/6/75	9/4/75	9/3/75	8/30/75	8/29/75
Well Collar to Reference[1]		295.6 ft	297.8 ft	300.5 ft	302.4 ft	297.3 ft	300.7 ft	298.7 ft	300.0 ft
Geophones	a	60.0	60.0	60.0	60.0	60.0	60.0	60.0	-
	b	50.0	50.0	50.0	50.0	50.0	50.0	50.0	-
	c	40.0	40.0	40.0	40.0	40.0	40.0	40.0	-
	d	30.0	30.0	30.0	30.0	30.0	30.0	30.0	-
	e	22.5	22.5	22.5	22.5	22.5	22.5	22.5	-
	f	15.0	15.0	15.0	15.0	15.0	15.0	15.0	-
	g	7.5	7.5	7.5	7.5	7.5	7.5	7.5	-
	h	0.0	0.0	0.0	0.0	0.0	0.0	0.0	-
	i	-10.0	-10.0	-10.0	-10.0	-10.0	-10.0	-10.0	-
	j	-20.0	-20.0	-20.0	-20.0	-20.0	-20.0	-20.0	-
Resistivity Probes	a	32.0	32.0	32.0	32.0	32.0	32.0	32.0	32.0
	b	16.3	16.0	16.0	16.0	16.3	16.0	16.0	15.0
	c	-2.0	-2.0	-2.0	-2.0	-2.0	-2.0	-2.0	-2.0
Thermocouple Levels (Low Temp)	a	74.6	73.9	73.1	74.1	72.0	74.2	74.3	-
	b	40.3	40.1	39.9	39.8	40.3	40.1	40.0	-
	c	30.5	30.2	28.1	30.0	30.4	30.2	30.2	-
	d	25.5	25.1	25.1	25.0	25.4	25.0	25.2	-
	e	23.0	22.7	22.5	22.5	23.0	22.6	22.0	-
	f	20.5	20.1	20.0	20.0	20.2	20.1	20.1	-
	g	18.0	17.7	17.5	17.6	17.8	17.7	17.0	-
	h	15.5	15.2	15.1	15.1	15.4	15.0	15.1	-
	i	13.0	12.7	12.6	12.6	12.9	12.6	12.0	-
	j	10.7	10.1	9.9	10.0	10.5	10.0	10.0	-
	k	0.0	10.0	0.0	9.9	10.2	0.0	0.0	-
	l	-	0.0	-	0.0	0.0	-	-	-
Thermocouple Levels (High Temp)	a	-	-	-	-	-	-	-	-
	b	-	-	-	-	-	-	-	-
	c	-	-	-	-	-	-	-	-
	d	-	-	-	-	-	-	-	-
Gas Sampling Canister		-	19.0	19.0	-	-	-	-	-
Pressure Transducer		-	-	-	-	-	-	-	-
Tilt Meters	a	66.0	66.0	66.0	66.0	-	-	-	-
	b	55.0	55.0	55.0	55.0	-	-	-	-
Displacement Gauge	reference	-	-	-	-	-	-	-	-
	a	-	-	-	-	-	-	-	-
	b	-	-	-	-	-	-	-	-
	c	-	-	-	-	-	-	-	-
	d	-	-	-	-	-	-	-	-

4. An extensive thermocouple array has been fielded. There is an increase in the number of thermocouple levels to improve spatial resolution within the coal seam. High temperature thermocouples have been emplaced in four wells. Three different state-of-the-art data acquisition systems will be used and evaluated. Approximately 90 selected thermocouples will be connected to LERC's process computer for their direct use; the special branched thermocouple circuits used will allow this to be accomplished on a non-interference basis.

5. In a few selected locations, downhole geophone amplifiers, high temperature resistivity probes and cables, and downhole pressure transducers have been fielded for evaluation.

6. Revised fielding procedures were adopted which include casing below the slough zone, a sequential drilling-fielding-grouting procedure, and the use of a continuously poured cement-flyash grout.

7. During different portions of the experiment, many wells should remain unaffected by the burn and will allow continuous downhole resistivity, passive acoustic, and induced seismic data to be obtained below, within, and above the coal seam. Well N and resistivity probes fielded outside the casing in Well S1 should not be affected during the life of the experiment.

8. Tilt meters and displacement gauges have been fielded in selected wells to provide information on the initial stages of subsidence in the formations above the coal seam. This is the first time such instruments have been fielded for this application.

Effectively, 12 different instrumentation techniques will be evaluated during Phase 2 and 3, and these have been summarized in Table II.

TABLE II

INSTRUMENTATION TECHNIQUES TO BE FIELDED AND EVALUATED ON THE SECOND HANNA IN SITU COAL GASIFICATION EXPERIMENT

		PHASE 1	PHASE 2	PHASE 3
THERMAL				
Low Temperature		X	X	X
High Temperature			X	
ELECTRICAL RESISTIVITY				
Resistivity	Surface and Downhole Arrays	X	X	X
Voltage Gradient	Surface and Downhole Arrays		X	X
Telluric Current	Surface and Downhole Arrays		X	X
PASSIVE ACOUSTIC		X	X	X
INDUCED SEISMIC				
Downhole-Downhole			X	X
Downhole-Surface			X	X
IN-SEAM GAS SAMPLING				
Composition		X	X	X
Pressure		X	X	X
DISPLACEMENT				
Near Overburden			X	X
TILT				
Near Overburden			X	X

IV. TEMPERATURE

A. In Situ Temperature Measurements

(S. G. Beard, 5732, and R. P. Reed, 1116)

The temperature distributions in Wells AA, BB, CC and DD during Phase 1 were presented and discussed in the Second and Third Quarterly Reports. During this quarter, temperatures in Wells AA and BB associated with natural and injected water quenching in the reaction zone were recorded intermittently and are presented in Figures 5-7. Temperatures were recorded electronically through September 19, (Day 261) when recording was terminated to allow preparation of the system for Phases 2 and 3.

Although the reliability of the temperatures at levels 6, 7, and 8 in Well AA for times after Day 239 has not been determined, during the initial quench period a definite cooling trend is evident within the seam (Figure 5). The temperature decrease for level 8 between Days 242 and 261 indicates that 7 or 8 months would have been required for the temperature in the reaction zone to decrease exponentially from 1010 to 60°F as a result of thermal conduction. The low level temperatures in Well BB (Figure 6) continued to increase slowly as a result of conduction and/or

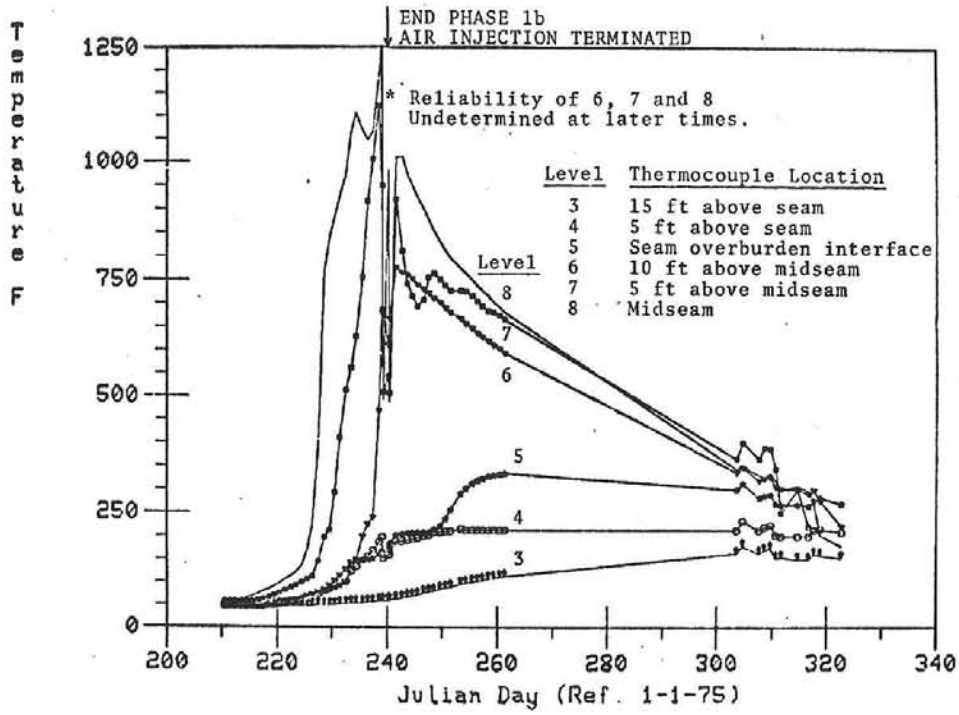

Figure 5. Selected Temperatures in Well AA During Phase 1b and Quench

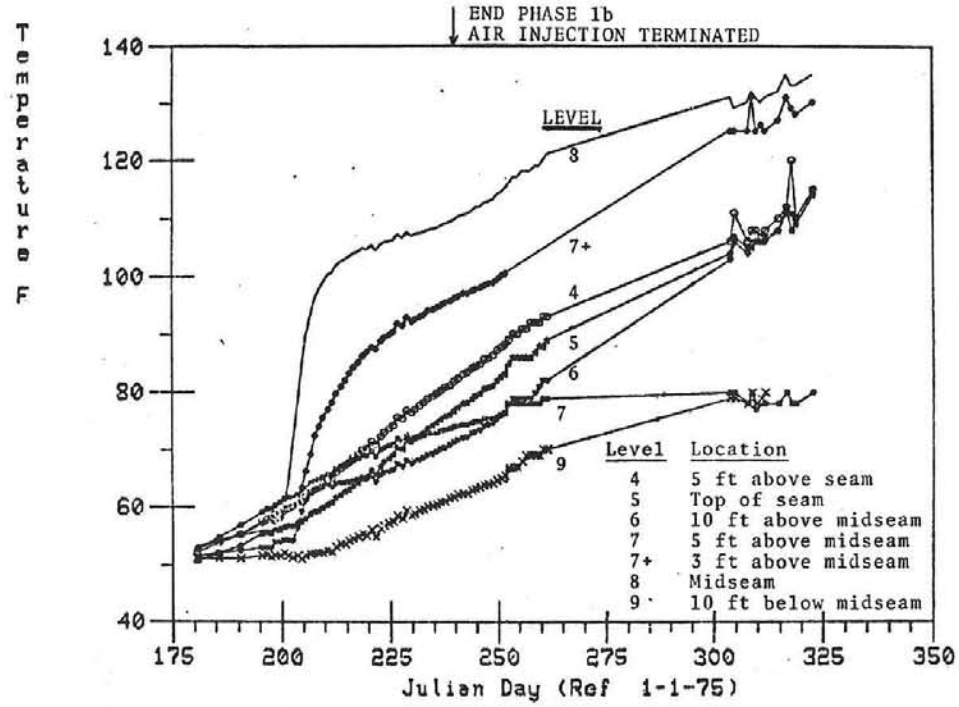

Figure 6. Selected Temperatures in Well BB During Phase 1b and Quench

fluid convection from the hot reaction zone considerably distant from this well. The daily data fluctuations following Day 303 probably resulted from the measurement of thermocouple temperatures with less precise, portable equipment during this period.

From Day 310 to Day 321, water was injected by LERC into the Phase 1 reaction zone to increase the rate of cooling prior to air injection in Phase 2. (There was concern that high pressure air injection into Well 7 could conceivably reach the Phase 1 region producing an undesired combustion link.) The water quenching resulted in increased rates of cooling at levels 6, 7 and 8 in Well AA, and by Day 322 temperatures in the reaction zone were less than those in the overburden immediately above the coal seam as shown in Figure 7.

Although the temperatures recorded for Well DD after Day 182 are in question, the indicated temperatures in this well have steadily decreased from ~1400°F at the end of Phase 1a (Day 192) to 225°F on Day 322. Temperatures in these Phase 1 instrumentation wells will continue to be monitored periodically during Phases 2 and 3.

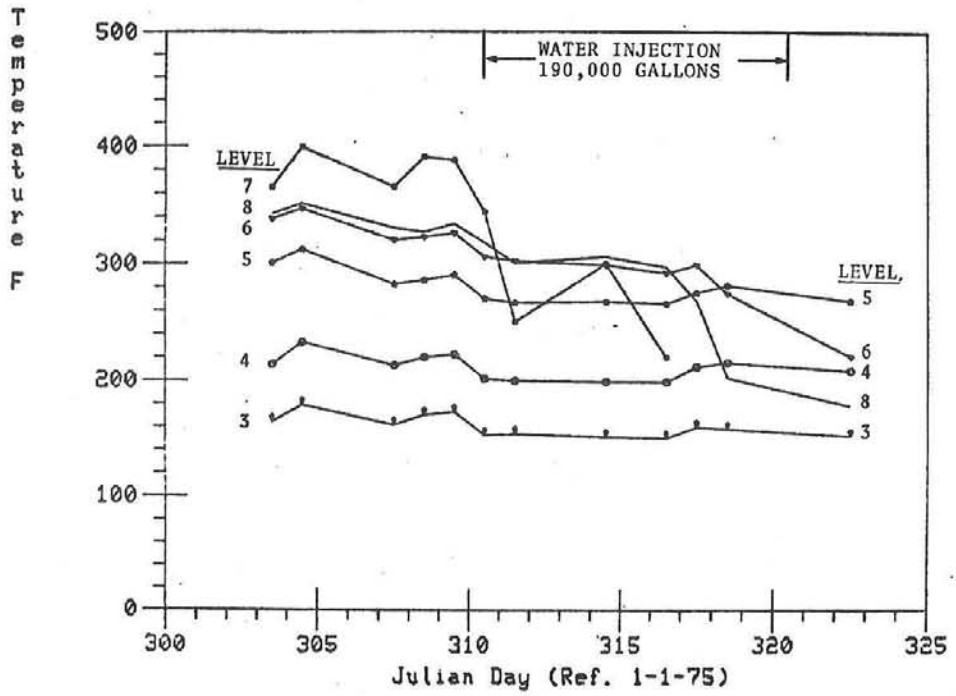

Figure 7. Temperatures in Well AA Immediately Before and During Water Injection.

B. Thermal Instrumentation (R. P. Reed, 1116)

The installation of the thermal instrumentation and well-to-trailer cables for Phases 2 and 3 was completed during this quarter. Temperatures will be measured at 169 locations in 15 wells. The relative positions of the thermal sensors are shown in Table III. The thermocouple locations extend from above the coal seam to the seam floor in all wells, and, in two wells, a thermocouple is located below the seam floor. The design of these thermocouple circuits provides up to six-fold redundancy at many locations and also incorporates diagnostic measurements of resistance and spurious emf. Although most of the temperatures will be measured with inconel-sheathed, chromel/alumel thermocouples as in Phase 1, some temperatures in Wells B, C, E and F will be measured with higher temperature platinum/platinum 10% rhodium and tungsten 5% rhenium/tungsten 26% rhenium thermocouples sheathed with platinum or molybdenum and insulated with MgO or BeO.

Three different commercial data loggers (Doric, Esterline-Angus, and Vidar) will be used to record the thermal data in order to increase the number of channels recorded and also to evaluate the three types of data loggers in the field environment. Sandia Laboratories will record 355 temperature and temperature-related diagnostics, and some data will be transmitted daily via a phone link directly to a Sandia computer in Albuquerque. Ninety temperature channels will be patched directly to the on-site LERC computer; these channels will include at least five temperatures in every well: coal floor, midseam, ceiling and two intermediate points. Redundant measurements of the temperatures transmitted to the LERC computer will also be recorded by Sandia. In Phases 2 and 3, the vertical resolution has been improved by the 2.5-foot spacing of the thermocouples in several wells, and some horizontal resolution is allowed by the well pattern shown in Figure 1.

During Phase 1, the quality of the temperature data was excellent, but some inconveniences in data handling resulted from faulty hardware. However, all expected data were obtained. Although the spatial resolution was limited, meaningful interpretations of the data were made in conjunction with LERC. The results of the thermal measurements were reported jointly with LERC at the Annual Society of Petroleum Engineers meeting in September. A more consistant master file of thermal data is being compiled that will provide versatile plotting and further analysis of Phase 1 data.

V. SEISMIC-ACOUSTIC STUDIES

A. Assessment of Passive Acoustic Techniques (L. W. Beckham, 5732)

Three signal types were observed during Phase 1. They were continuous burning noise (only once) and the two discrete signal types, Type A and Type B, as discussed in the last quarterly. The continuous burning noise and signals of Type B are useless for source determination due to their infrequent occurrence and poor signal to noise ratio. In addition, for Type B data, the overlap of various events in time precludes the determination of the spatial origin of the data.

TABLE III

VERTICAL PLACEMENT OF TEMPERATURE SENSING POINTS RELATIVE TO INSTRUMENT REFERENCE AT INSTALLATION

WELL

LEVEL NOTATION	NOMINAL LOCATION (feet)		LOW TEMPERATURE															HIGH TEMPERATURE			
			A	B	C	D	E	F	O	G	H	I	J	K	L	M	N	B	C	E	F
2+	0-30		5.7	10.7		15.9			27.1		5.4	6.1	6.9	5.9	6.0	5.8	5.7	15.0	15.0	15.0	15.0
3	35																				
	37.5																				
3+	40		40.0								39.7	39.9	40.1	40.2	39.7	39.9	40.0				
	42.5																				
4	45			44.9	44.8		45.0	44.5	44.8	44.7											
4+	47.5			47.5	47.3																
5	50		49.8 50.0	~50.0	49.8	49.8 50.0	49.7	49.7 49.8	50.0	49.4 49.6	49.5	49.8	51.9	50.0	49.6	49.8	49.8				
5+	52.5	COAL SEAM		52.3																	
6	55		54.8		54.9		55.0	54.8	55.0	54.7	54.5	54.9	54.9	55.0	54.6	55.0	54.8				
6+	57.5		57.5	57.4							57.0	57.3	57.5	57.5	57.0	57.4	~58.0				
7	60		59.9		59.9 59.9	59.8	59.8 59.9	59.8 59.8	60.0	59.8	59.5	59.9	60.0	60.0	59.8	59.9	59.9	60.0 60.0		60.0 60.0	59.8 59.8
7+	62.5		62.4	62.1							62.0	62.3	62.5	62.4	62.2	62.3	~63.0				
8	65		64.9	64.8	65.1	64.9	65.0	64.5	65.1	64.4	64.5	64.8	64.9	64.9	64.6	65.0	64.9	65.0	65.0 65.0	65.0 65.0	64.0 65.0
8+	67.5		67.5	67.5		67.3					67.0	67.3	67.4	67.4	67.1	67.4	~68.0				
8*	70		70.0		69.5	69.9	70.0	69.9	69.7	69.6	69.3	69.9 70.0	70.1	70.0 70.1	69.5 69.8	70.0	70.0				
8)	72.5					72.3															
9	75			74.8	75.0	74.8	74.9	74.9	75.0	74.7											
9(	77.5					77.2															
9+	80		80.0	79.8	80.1	79.8	80.0	80.0	80.0	80.0	80.0	80.0	80.0	80.0	80.0	80.0	80.0				
9*	82.5			82.4																	
	85																				
	87.5																				
9)	90					90.0															

Signal Type A is more amenable to analysis. This signal type occurs predominantly in the overburden as determined from signal levels and several triangulations. This activity is associated primarily with the gasification phase and not linkage as seen by a histogram of observed frequency of Type A signals shown in Figure 8. The major seismic phase generated by signal Type A appears to be SV, with P waves contributing much less to the total received signal. Using the previously determined average compressional wave attenuation coefficient of 0.04 db/ft* and the fact that shear wave attenuation is an order of magnitude greater, an appropriate average attenuation coefficient for Type A signals is 0.4 db/ft. Given that signal level maxima observed to date are 10^{-3} in/sec at a source to receiver distance of 20 feet and that the background noise level is 10^{-5} in/sec, one may assume that a usable signal to noise ratio of 10 will result if a geophone is placed at a distance of 50 feet from the focus of the event. This result is determined by using the relation

$$rA = r_o A_o 10^{-\alpha(r-r_o)/20} ,$$

where α is the attenuation coefficient, A_o is the signal amplitude at some arbitrary starting point r_o (here r_o = 20 feet) from the source, and A is the amplitude at distance r.

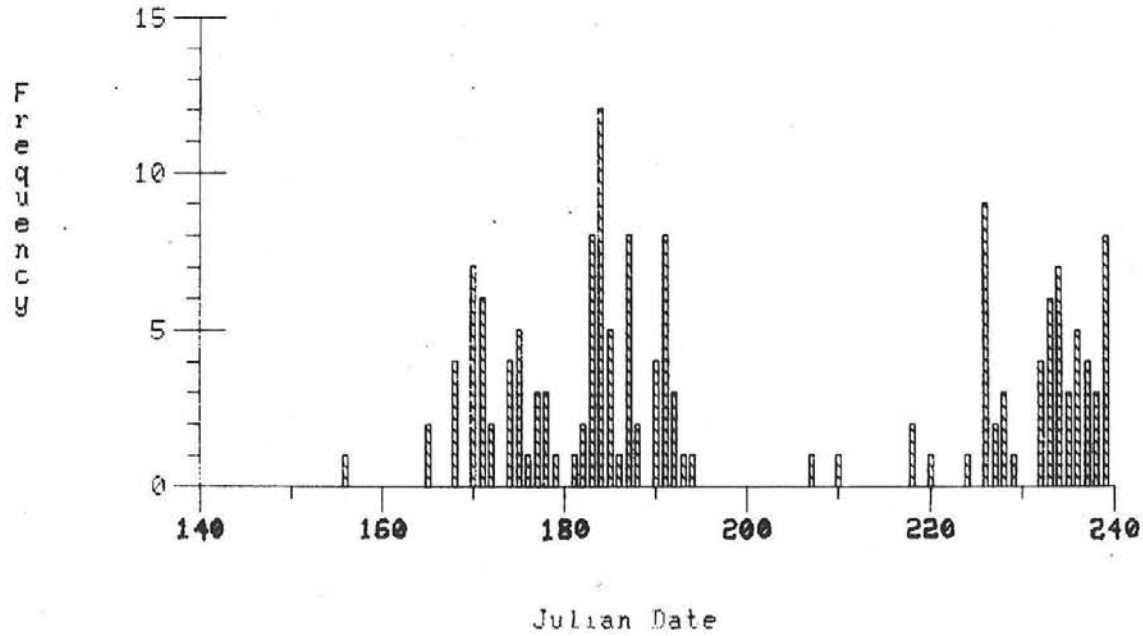

Figure 8. Frequency of Type A Signals During Phase 1 (Number per five-minute interval received in enough channels to allow triangulation.)

* S. D. Stearns, "Attenuation of Acoustic Compressional Waves in Coal and Shale at Hanna, Wyoming," Sandia Laboratories Report, SAND-75-0471, November 1975.

The above result requires that geophones be emplaced fairly close to the area of interest for useful results. Note that one possible solution to poor signal to noise ratios is the use of downhole geophone amplifiers since the background noise appears to be mainly electronic and/or mechanical within the tape recording system. This approach will be tested during Phase 2 via the installation of downhole geophone amplifiers in Wells A, F, G. In addition, geophones in Well G have been equally spaced from below the coal seam to just below the well casing. This is to provide more reliable information on the attenuation of vertically-traveling passive signals than is presently available.

Several source locations using Type A data from Phase 1a (Days 168 and 171) were obtained by visually inspecting the data for times of arrival. These locations are shown in Figure 9. In addition, attempts were made to cross-correlate data in the various channels to obtain differential times for source locations purposes. The success of this operation depends on (a) the similarity of the signals as they appear in the various channels, (b) the overlap of P and S wave types, and (c) the reasonably accurate determination of the different sonic velocities within the region of interest. To some extent, dissimilarity of the time character between channels due to multipath effects can be corrected with low pass filtering. However, the resulting differential time may not be easily determined because of the complicated nature of the cross-correlation function. Techniques to correct the above problems are being considered. In the event that they can be corrected, an automated detection, correlation and source location code will be developed.

Based on the limited data base from Phase 1 and the source locations obtained to date, the passive acoustics approach is considered to be feasible in providing some data suitable to process control. Given an expanded data base during Phase 2 and success with an automated source location and display operation, this technique may provide valuable insight as to the extent of the gasification process.

B. Induced Seismic Experiments, Phases 2 and 3

(L. W. Beckham, 5732, and H. D. Garbin, 1111)

Downhole and surface geophones have been installed at locations defined in Table I and Figure 4. Replaceable, twelve-detonator strings in Wells S1 and S2 will provide the signal sources for the downhole-to-downhole measurements. Larger detonators will be used at 350-450 ft depths in S1 to shoot to the near-surface ($\sim$ 20-ft depth) geophone array to evaluate the downhole-to-surface technique.

Pretest data was collected during the last three weeks of November. Squibs were fired on the gas sampling canisters of Wells B and D for the purpose of velocity determination within the seam. These detonators were located approximately 19 feet above the coal seam floor in both wells. In addition, a set of twelve detonators were fired in Well S1 for the purpose of channel gain determination. Gain determination was necessary due to the unknown source to medium coupling for the detonators as well as the various shot locations. Then, using these preliminary gains, two sets of twelve detonators each were fired in Wells S1 and S2. These data will provide baseline amplitude, time of arrival and attenuation data for the experiment.

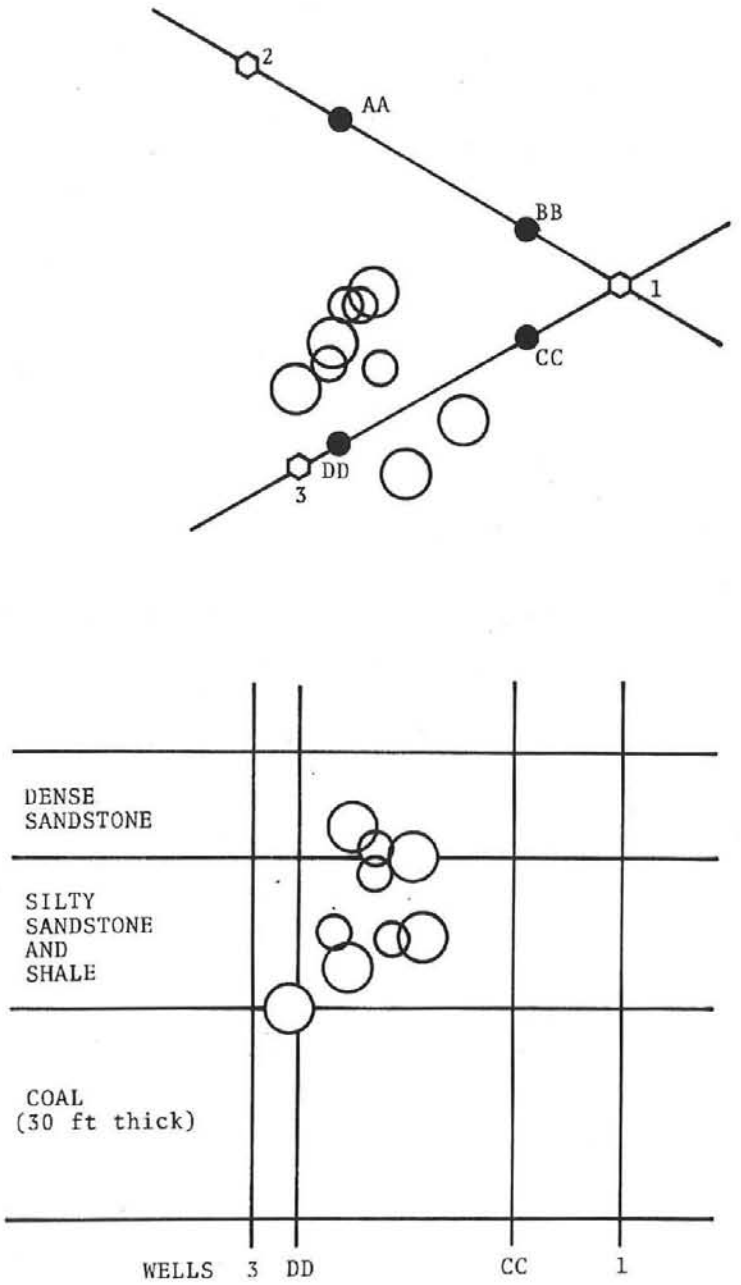

Figure 9. Source Locations for Selected Discrete Signals Recorded During Days 168 and 171, Phase 1a.

A computer code developed for the purpose of allowing quick access to all data in all channels during the course of the experiment has passed a preliminary check.* This program will, when merged with others under development, provide time of arrival, amplitude and spectral analysis of the approximately 3500 signals to be collected on any one firing day of the experiment.

C. Refraction Calculations (H. D. Garbin, 1111)

Velocity logs made in Well S1 indicate two high velocity, well-consolidated sandstone layers occur above the coal seam at depths of approximately 180 and 210 ft. The peak velocities measured in these two layers were 20,000 and 13,000 ft/sec, respectively. This has caused speculation that the energy transmitted to the outer surface geophone array (260 ft from Well S1) would be negligible due to refraction of the induced signals at angles greater than the critical angle (as measured from the normal). For a nominal velocity of 8000 ft/sec, these critical angles are 23.6° and 38.0° for the upper and lower layers, respectively (e.g., arc sin 8000/20000 = 23.6°). For shot-to-geophone depths of 330 and 430 ft, the approximate incident angles to the outer array are 38.2° and 31.2°, respectively (e.g., arc tan 260/330 = 38.2°). Thus, according to ray theory, the rays would be refracted along the upper sandstone layer.

Calculations were made to determine how much this layer does effect the transmitted energy. Fluid layers have been assumed and no mode conversion has been taken into account and, thus, the results may be optimistic. The results are shown in Figure 10; the transmitted/incident energy ratio has been plotted as a function of incident angle for frequencies of 225 and 550 Hz. These frequencies were selected because they were the predominate frequencies seen in previous surface and downhole shot records obtained during Phase 1. The high velocity layer acts as a low pass filter; the transmitted energy decreases with increasing incident angle and is more pronounced with increasing frequency. This low pass filtering effect will be an inhibiting influence on the analysis by causing reduced resolution. The inner surface array (145 ft from Well S1) should not be as affected as its incident angles for shot-to-geophone depths of 330 and 430 ft are 23.7° and 18.6°, respectively (e.g., arc tan 145/330 = 23.7°). In addition, diffraction theory indicates that energy will be transmitted through these high velocity layers at angles greater than the critical angle but that the energy will be greatly attenuated.

D. Simulation Studies (A. G. Beattie, J. C. Bushnell, and J. H. Gieske, all 9352)

Work has been started on a simulation of induced seismic techniques for location of the burn region in the Hanna in situ coal gasification experiment. The basic problem attacked by the study is the resolution obtainable in the acoustic mapping of a layered structure bounded on two sides by linear arrays of transducers,

---

* Developed by R. E. Jones, Division 2642, Sandia Laboratories.

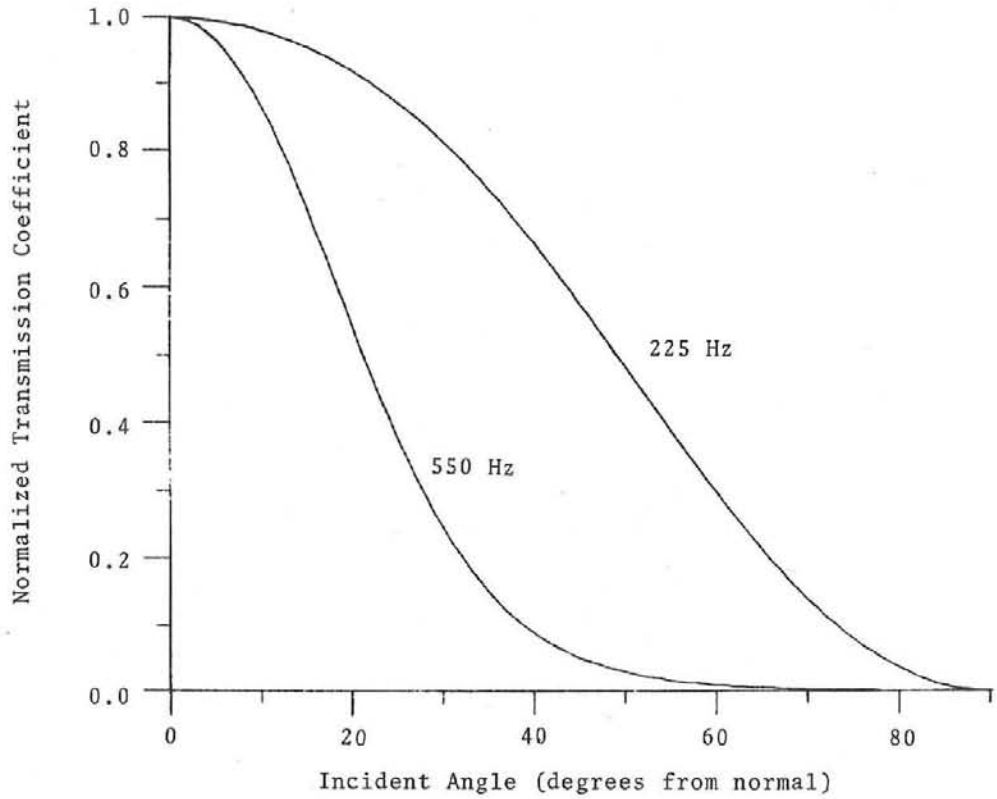

Figure 10. Normalized Transmission Coefficient for Different Frequencies as a Function of Incident Angle.

one transmitting and one receiving. A complicating factor in such an acoustic mapping is the frequency dependent attenuation of the coal. Data from Phase 1 indicates that the maximum usable frequency is around 500 Hz. At this frequency, the coal seam is less than two wavelengths thick, which may invalidate any mathematical model based solely on geometrical optics. The inclusion of diffraction effects in a model capable of giving reasonable results with data obtained in the field appears to be a formidable task.

These complicating factors dictate a two-pronged approach to the problem. An analysis initially based solely on a geometric optics approach is underway. To test this analysis, a physical model of the coal seam is being built. This model will attempt an accurate representation of the acoustic velocities and impedances, but not attenuation characteristics, of the layer of coal and adjacent rock layers. The model is scaled to preserve the wavelength/dimension ratios found at Hanna. It is hoped that this model will indicate how applicable the geometric optics approach is and will give guidance in including diffraction effects in the analysis.

E. Hardware Development for Data Collection and Transmission (T. M. Schultheis, 9423, and L. W. Beckham, 5732)

In order to provide rapid access to induced seismic data during Phases 2 and 3 and to test the feasibility of an on-site to Albuquerque data transmission system, a hardware configuration has been defined which will determine time of arrival, first peak amplitude and sign of the data signal for twenty-seismic-acoustic channels. The basic system is an add-on to the present system and procedures: it will tap data lines as they enter the instrumentation trailer, amplify and band-pass (adjustable) the geophone signals, determine the three parameters just mentioned, and store the resulting data on a TI 742 TTY with cassette option. Data would then be transmitted over existing phone lines to Sandia and into a similar computer terminal or the PDP-10 time sharing system for analysis. Pretest data collected at Hanna during November will be used to verify the feasibility of the hardware as well as validate system operation. Along present schedules, hardware construction and implementation should be complete by mid-March 1976.

A secondary purpose for the implementation of this hardware will be to test whether or not a simple threshold device can detect the passive signals observed at Hanna to date. If this is so, the system could become a basic building block for an overall process monitoring device.

VI. ELECTRICAL STUDIES

A. Mathematical Modeling of the Electrical Measurements (L. C. Bartel, 5732)

Electrical methods are being investigated as a possible means for monitoring the reaction zone during in situ coal gasification. The model for the electrical measurements results in solving for the nodal electrical potentials in a resistance network chosen to represent the overburden, coal seam, reaction zone, and underburden. The solution to the set of simultaneous linear algebraic equations is accomplished using matrix techniques and utilizing a so-called banded solver. The model has been discussed in Section VI-A, Second Quarterly Report, and Section V-A, Third Quarterly Report.

In this report, illustrative calculations of electric fields (or resistivities) will be given where the presence of the injection, recovery, and instrument wells is taken into account; these calculations differ from those reported earlier. In this case, the air injection drives the ground water from the coal creating a region of relatively cool, dry, unaltered coal with an assumed high resistivity (ρ) of 2.5×10^5 ohm-m. This high resistivity coal is assumed to be 9 m wide, extending 4.5 m outside the injection and recovery wells, and has the height of the coal seam, as shown in Figure 11. Surrounding this dry, unaltered coal is the wet, virgin coal bed with $\rho = 200$ ohm-m. The low resistivity, hot carbonized coal path, with an assumed $\rho = 5$ ohm-m, is taken to be 3 m wide with the height of the coal seam (9.2 m) and assumed to grow from the recovery well toward the injection well. In all the calculations, the electric field (or resistivity) is calculated for the virgin bed

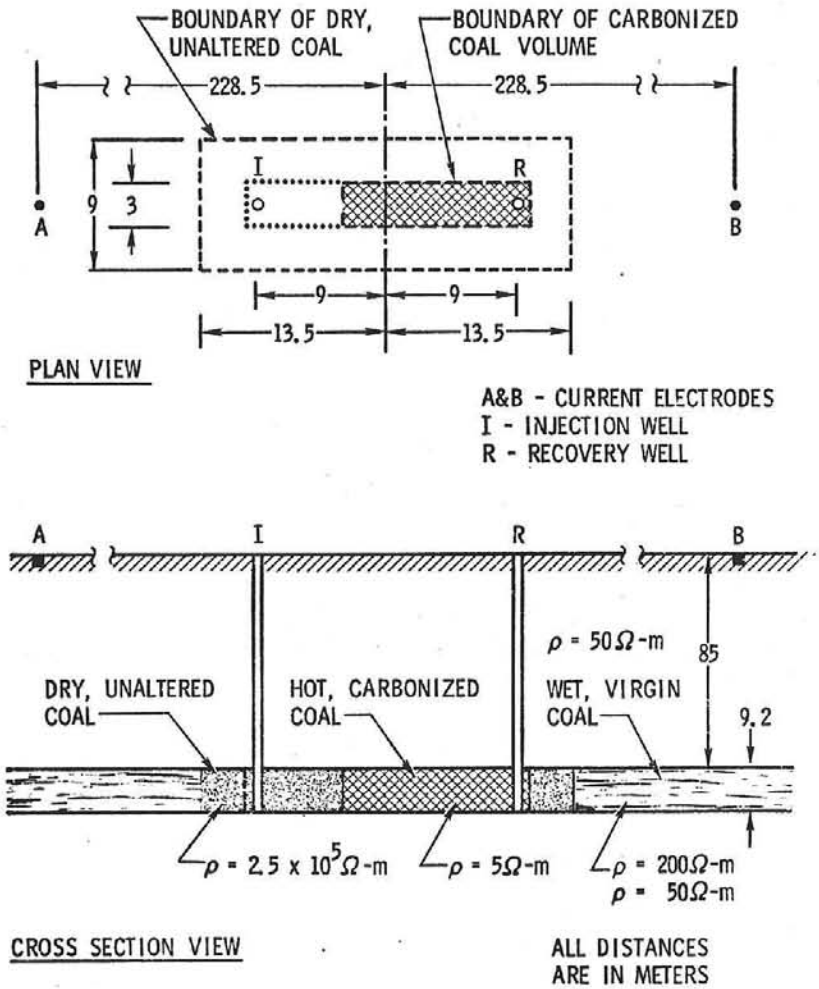

Figure 11. Schematic Layout for the Model Calculations

(VB) before air injection, after air injection which creates an island of dry, unaltered, high resistivity coal (UC), and during the growth of the low resistivity carbonized coal path. The low resistivity path could be a result of ash and void surrounded by hot, carbonized coal. The dimensions of the high resistivity island are assumed to remain fixed during the growth of the carbonized path within this island.

Figures 12 and 13 show the results of calculations for $|E_x|/I$ vs x on the centerline between the injection and recovery wells and 3 m off centerline; here I is the total current. The inset in each figure shows the location of the carbonized path and the location of the wells; in Figure 12 there are no instrument wells and in Figure 13 the instrument wells are in the carbonized path as shown. Finally, Figure 14 shows results of $|\Delta\phi|/I$ vs time for the potential difference ($\Delta\phi$) calculated

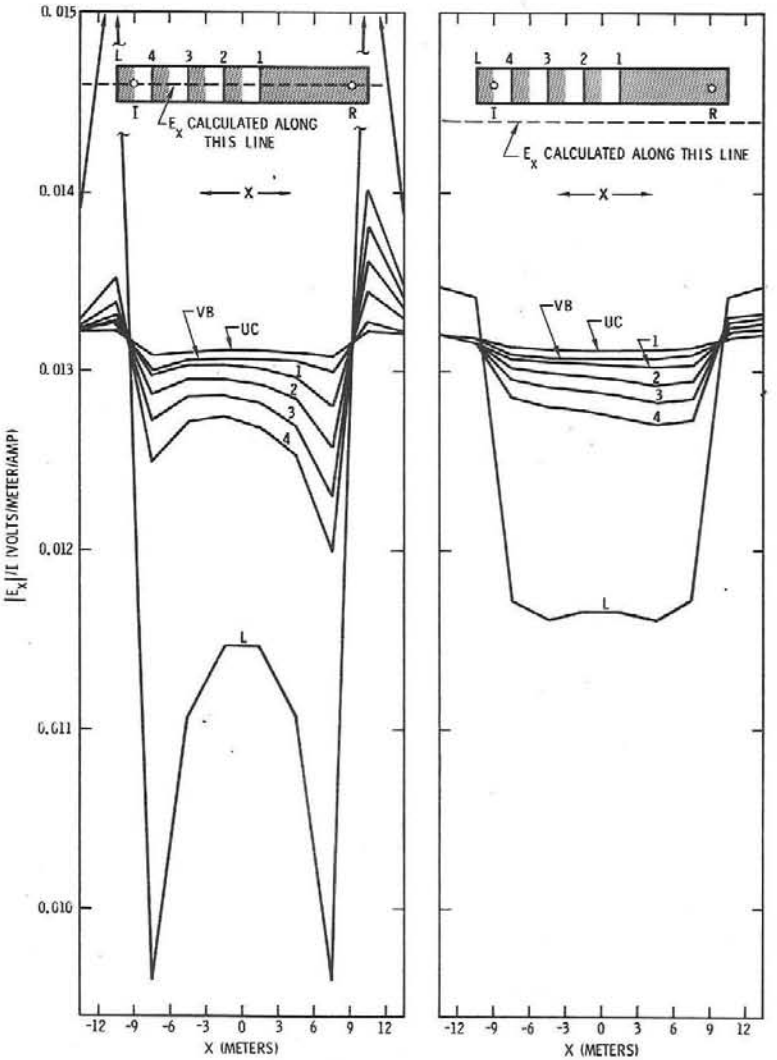

Figure 12. $|E_x|/I$ versus x Measured at the Surface with No Instrumentation Wells Present

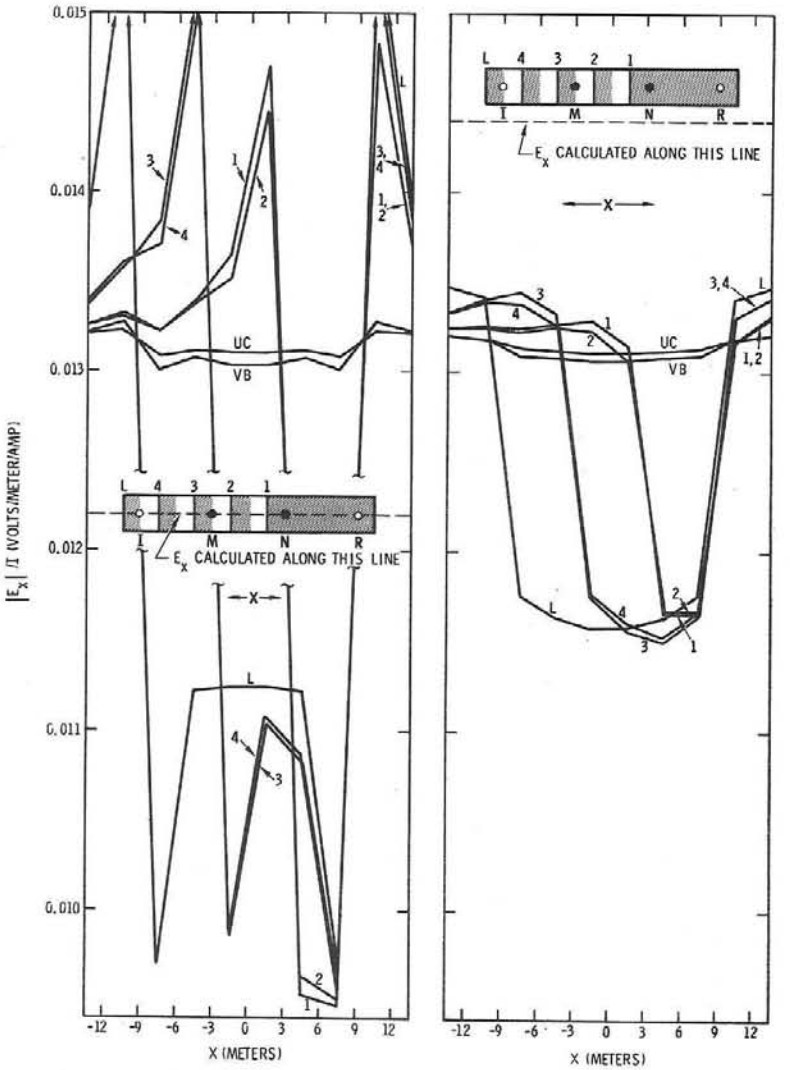

Figure 13. $|E_x|/I$ versus x Measured at the Surface with Two Instrumentation Wells Present.

(NOTE: Insets show the location of the hot carbonized coal paths at different times, the well locations, and the transverses of E_x on and 3 m off centerline.)

for probes at mid-seam in the instrumentation wells shown and assuming the probes would survive. Figures 13 and 14 represent the probe and well configuration for measurements made during Phase 1.

From knowledge of the behavior of electrical currents and from the calculations, the following physical picture for the behavior of the electric field emerges. The island of high resistivity, dry, unaltered coal (UC phase) repels the electric fields lines forcing some of them into the overburden and hence leads to larger electric fields at the surface than in the VB phase. The $|\Delta\phi|/I$ (resistivity) determined by probes at mid-seam in the coal is also larger in the UC phase than in the VB phase. As a low resistivity, hot carbonized path grows, electric field lines are "pulled" into this volume leading to a decrease in $|E_x|$ at the surface. When the low resistance path is at least partially between the instrument wells, the effective resistance decreases for the mid-seam $|\Delta\phi|/I$'s. The low resistance paths from the coal seam to the surface via the wells provide "communication" to the surface by distorting the electric field. When a low resistance path is provided between wells in the coal seam (electrical linking), a large amount of current flows in the seam leaving less to flow at the surface; hence, the large decrease in $|E_x|$ at the surface when electrical linking occurs. In this last case, where a large current flows in the coal seam, the $|\Delta\phi|$ between instrument wells in the seam is reduced even though there is an increase in current; this is because the resistivity is significantly less than in the UC phase. The value of $|\Delta\phi|$ in the carbonized path is a result of the competition between an increase due to increased current and a decrease due to a decreased resistivity.

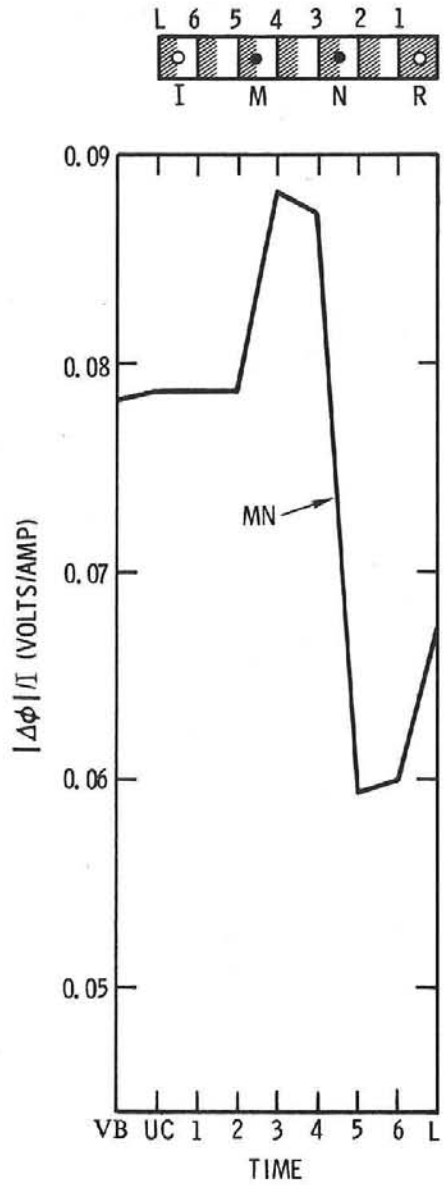

Figure 14. $|\Delta\phi|/I$ at Midseam as Measured Between Wells M and N as a Function of "Time" for the Carbonized Path Locations Shown in the Insert.

From the limited number of model calculations which have been done, it appears that the surface and subsurface electrical measurements may be used to locate and

monitor the reaction zone for in situ coal gasification. Clearly, from the calculations, each particular case would need to be modeled because placement of the instrument wells is important.

B. Interpretation of Phase 1 Electrical Resistivity Data

(L. C. Bartel, 5732, and R. W. Seavey, 5733)

Electrical resistivity data from Phase 1 of the Hanna II in situ coal gasification experiment have been reduced for the time period from Day 118 to 236, which essentially covers all of Phase 1. Examination of the resistivity record indicates several periods of unusable data: (a) Day 123-130, circuit interruption, (b) Day 178-184, faulty calibration battery, (c) Day 184-192, lightning damage, and (d) Day 225-231, instrument calibration error. In addition, further analysis has shown no correlation between the sharp drop in current on Day 155 (as shown in Figure 22, Third Quarterly Report) and resistivity and the drop may be due to a change in contact resistance. The field data are noisy and show considerable variations which are believed due to telluric currents and changes in surface conditions. In Phases 2 and 3, signals will be referenced to gauges located outside the test area so that trends and differences may be more apparent.

Figure 15 presents data for three selected surface probes during Phase 1. These probe pairs are located near Well AA (00030004), near Well DD (00220023), and midway between (00130014); the midpoints of these selected pairs are shown in Figure 16. The Third Quarterly Report includes all probe locations (Figure 1) and a discussion of salient Phase 1a (Day 118-192) features in the data. Two features during the Phase 1b period (Day 192-240) are of interest here.

(a) A distinct resistivity dip was measured in gauge 00030004 on Day 205. This feature occurs shortly after combustion linkage (Day 203) of Well 2 to the combustion region between Wells 1 and 3 and corresponds to the time that the probe pair below the coal seam between Wells AA and BB was destroyed (i.e., cables above the probe would be unreliable above 300°F). From the model calculations, this dip is indicative of electrical linking and, in this case, probably to the messenger cable in Well AA. This suggests that combustion linkage occurred near the bottom of the coal seam near Well AA. There were no thermocouple locations below midseam in this well and temperatures at midseam did not rise until Day 211 and went above 300°F on Day 227. The slight dip seen in gauge 00220023 at this time is possible since the conductive gasified region extends under this location as well.

(b) There was a general increase in the resistivity from Day 200 to Day 218. During this time, a small peak was recorded on Day 211 for all reliable surface gauges; the amplitude was smallest for the gauges in the southeast corner of the array. The time corresponds to a step increase in injected air flow and pressure. This general increase in resistivity is believed due to the growth of the burn region and the

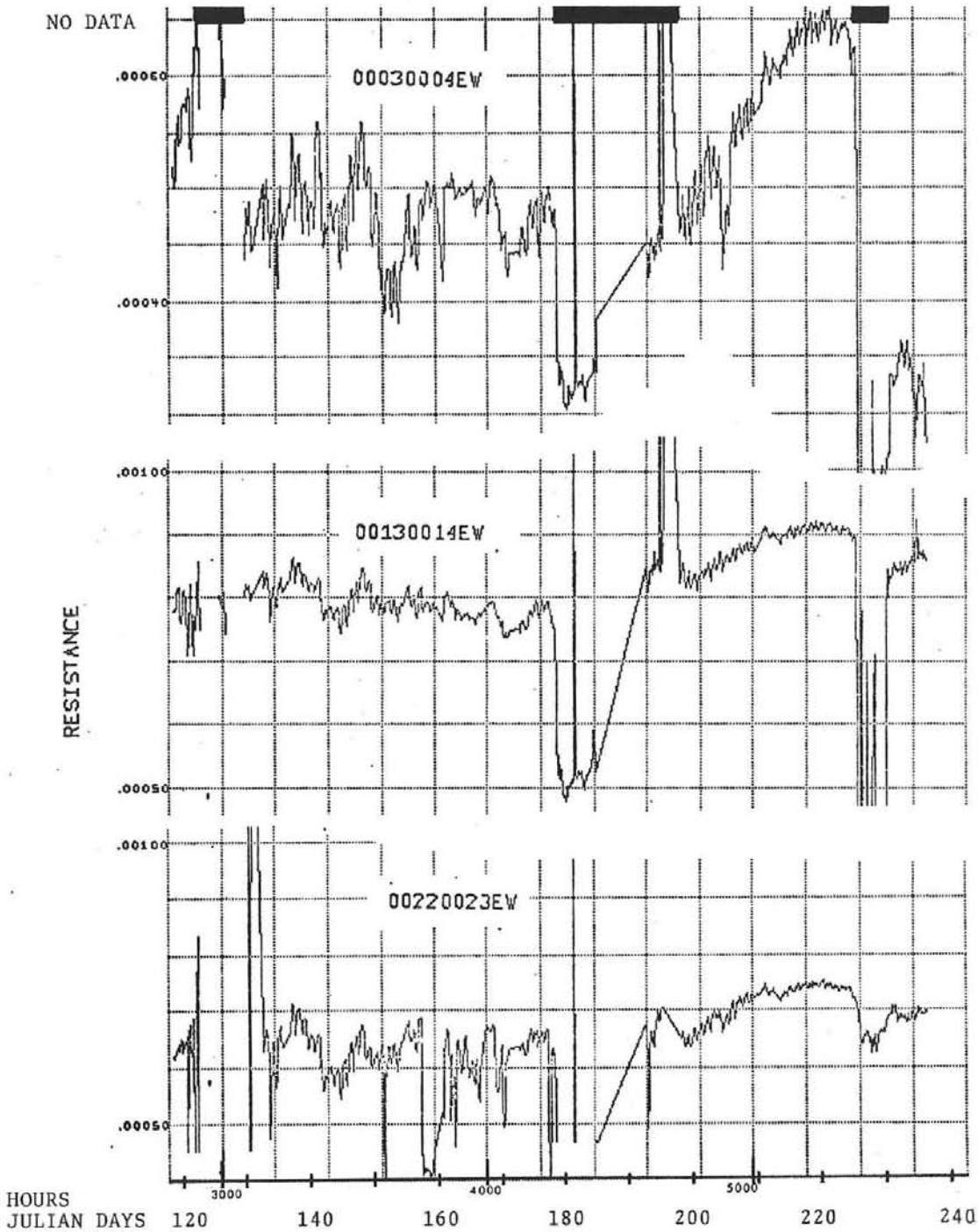

Figure 15. Observed Resistivity for Selected Surface Gauge Locations During Phase 1.

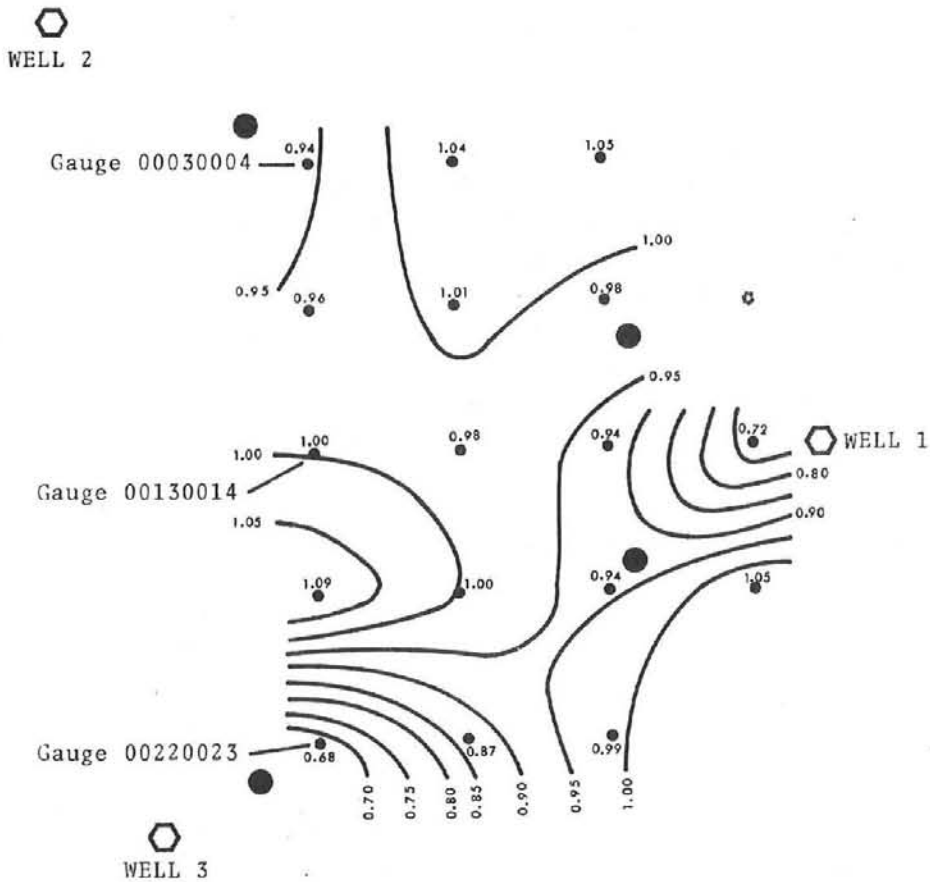

Figure 16. Plot of Surface Resistivities Measured on Day 158, Phase 1.

general drying out of the surrounding coal, thus increasing its resistivity. Competing with this rise and possibly causing the maximum at Day 219, is the decrease in resistivity due to the creation of regions of hot carbonized coal of low resistivity which surround the ash and void produced by gasification.

A representative contour plot for the limited surface array is shown in Figure 16. Codes to present the data in this convenient manner are being investigated. Reduced resistivity (resistivity/resistivity on Day 119) data are shown for Day 158 which is shortly after the electrical linking between Wells 1 and 3. The plot shows a relatively uniform resistivity under the upper portion of the array, and a saddle under the lower portion of the array. The saddle and the relatively low resistivity path between Wells 1 and 3 suggest the general direction of the combustion link which could not be detected thermally in Well DD. This saddle feature is consistant with the calculations shown in Figures 12 and 13 for times after electrical linking between wells.

C. Electrical Instrumentation, Phases 2 and 3

(R. W. Seavey, 5733, and L. C. Bartel, 5732)

Several changes have been incorporated into the plans for the electrical measurements for Phases 2 and 3; these changes have been based upon experience and data from Phase 1 and the concurrent mathematical modeling studies. Three separate measurements will be made: resistivity, voltage gradient, and telluric current. All three techniques will be measured at the surface (an 80 probe array emplaced at a depth of 6 ft, as shown in Figure 4) and downhole (three probes nominally located at midseam and 2 ft above and below the seam in each instrumentation well and outside the non-conductive casing in Well S1). The resistivity technique is similar to that fielded in Phase 1: current will be induced into two 30-ft cased wells (P and R) lying 750 ft on either side of Well C along the S1-N line. The voltage gradient technique will use Well 5 as one of the current sources and potential gradients will be measured. Thus, this current source will be in direct contact with the burn area and the current electrode's geometry will change with the burn itself. The other current well in this case is the west current well (T) used in Phase 1 and is located on a bearing of S72W and approximately 590 ft from Well 5. The third technique consists of recording the voltages produced in the probes due to naturally-occurring telluric currents rather than an induced current.

Other features of this revised instrumentation plan include:

(a) A set of four surface probes has been fielded well outside the burn area to measure potentials due to changes in telluric currents and surface conditions. These baseline data will be used to normalize the other data, thus reducing the daily fluctuations and periodic changes observed in Phase 1.

(b) Measurements will be made to a common surface probe and downhole probe. This allows more data to be obtained for a given number of recording channels and provides for greater flexibility in the subsequent data analyses.

(c) High temperature resistivity circuits have been fielded in Wells E and F. These circuits have stainless steel probes and inconel-sheathed, magnesia-insulated wire through, and to well above, the coal seam.

(d) The downhole resistivity probes in S1 and Well N are expected to remain outside the burn area for the duration of the experiment. Further, Wells H-N should be unaffected during Phase 2, allowing the more sensitive downhole probes to be active throughout that phase.

(e) There are more probes than recording channels. Junction boxes have been included in both the surface and downhole circuits to provide maximum flexibility in the recording. Different patches have been designed for different portions of the experiment.

VII. SUPPORTING STUDIES

A. Grout Properties and Behavior (S. G. Beard, 5732, Coordinator)

The grout used in the instrumentation wells forms the interface between the coal, surrounding formations, or reaction zone and the instrumentation, and therefore, the integrity of the grout column is an important factor in most of the techniques fielded. Thus, the properties and behavior of the grouts used in Phases 1, 2, and 3 are being investigated in the laboratory.

Samples of the Phase 1 coal-filled grout were heated to 550°C in air for three hours; an overall 60% weight loss was noted for the sample which originally contained 35.0% coal, 24.1% cement, 33.8% water, and 7.1% fine clay. The resulting sample was a lightly consolidated material with little strength and with no coal remaining. These results suggest that the grout column surrounding the thermocouples as fielded in Phase 1 could slough away very early during gasification. The thermocouples would then be exposed to gas flows and rapid temperature fluctuations could be observed which are not representative of the temperature of the surrounding solid materials. Thus, the transient response of the thermocouple junctions which have and will be fielded at Hanna were also examined in the laboratory. Response times of 50 and 110 sec to 99% of a 70°C step increase were measured for two junction designs. Conduction calculations indicate that the fastest transients which can be observed by junctions embedded in the solid is on the order of a few minutes. Where the junctions are "bare" in a cavity, response times can be very much greater. These results affect the choice of sampling frequency.

A more extensive study of the Phase 2 grout (~70% cement, 30% flyash composition) is being conducted. Thermogravimetric analyses and the measurement of thermal conductivity to 267°C have been completed. The thermogravimetric analyses indicated overall weight losses of 18 and 26% at 300 and 1200°C, respectively; most of this loss occurred at ~100°C and is assumed to be water.

The following measurements will also be made: specific heat, expansion and shrinkage as functions of temperature; room-temperature tensile and compressive strengths of samples which have been heated to temperatures as high as 1000°C; and mechanical strengths as a function of temperature over a limited temperature range. Thermocouple and grout response will be studied in an experiment in which a grout-enclosed thermocouple string is heated during coal gasification in a reaction tube. Preliminary results for a sample heated to 1000°C indicate that the strength and integrity of this Phase 2 grout is significantly greater than that of the Phase 1 coal-filled grout. However, the heat-treated sample shrank ~7.5%, and extensive crack patterns (1 to 2 cracks per inch) were observed in the exterior surface.

B. Thermal Conductivity of Core Samples (R. U. Acton, 5842)

The thermal conductivity of coal, overburden and grout are to be measured. A new experimental apparatus is being checked out which will allow the cores to be measured without requiring extensive machining. The apparatus will accept cores

having had only the ends squared off and a few thermocouple holes drilled. Another advantage of the new apparatus is that the data will be more representative of the parent material because of the large sample size.

To date, cores of grout have been measured. The materials are of the 70/30 and the 50/50 cement/flyash composition. When drilling the thermocouple holes, it is found that the outer portion of the material is dry and powdery whereas the inner portion is wet and muddy and cakes onto the drill. During the measurement of thermal conductivity, the water redistributes itself due to the thermal gradient and finally dries out. The composition of the material thus changes during the determinations. The data for these two grouts are shown in Table IV. It should be noted that there is a break in the data near 200°F which can be attributed to drying.

These data are considered preliminary. The heat transfer computer codes HEATMESH and CINDA are being used to analyze the heat flow patterns in the experiment. These will be studied as a function of core size, core conductivity and temperature in order to determine if systematic errors exist.

TABLE IV.

THERMAL CONDUCTIVITY OF GROUT: PRELIMINARY DATA

Temperature		Cement/Flyash Ratio			
		70/30		50/50	
K	°F	W/cm K	Btu/hr ft°F	W/cm K	Btu/hr ft°F
334	142	0.0071	0.41		
345	162	0.0067	0.39		
365	197	0.0029	0.17		
380	225			0.0045	0.26
392	247	0.0026	0.15		
407	274			0.0038	0.22
456	362	0.0019	0.11		
540	512	0.0017	0.10		

C. Specific Heat of Hanna Coal (H. P. Stephens, 5842)

The specific heat of a sample of Hanna coal has been determined from 335 to 600 K by differential scanning calorimetry. The coal sample was a portion of a core section taken from Well 2 at a depth of 285 ft. The core had been placed in a polyethylene wrapper and stored out-of-doors for several months prior to measurement.

Differential scanning calorimetry samples were prepared by pulverizing and thoroughly mixing several grams of the core and drying this powder to constant weight at ~ 370 K. During the drying process, the powder lost 4.4% of its initial weight.

Before the specific heat measurements were made, a thermal scan of the coal sample was made to 700 K. A slightly endothermic process was found to occur between 380 and 530 K (possibly vaporization of tightly bound moisture or very volatile hydrocarbons), and gross devolatilization of the coal occurred at 640 K.

The results of the specific heat measurements are given in Table V. The sample was re-weighed after each measurement. Since the sample lost weight with increasing temperature, the specific heats are based on the sample weight taken after each measurement. The probable error in the specific heats is no greater than ± 10%. These data are found to compare closely with published values for the specific heat of coal with a volatile content of 35%.*

TABLE V.

SPECIFIC HEAT OF HANNA COAL

Temperature (K)	Specific Heat (cal gm^{-1} deg^{-1})	Weight (mg)
335	0.35	34.0
400	0.36	33.9
500	0.44	32.9
600	0.47	31.9

(R. E. D. Stewart and J. A. Allensworth, both 5742)

D. Systems Studies

1. Brayton Cycle Analysis:

A new computer routine incorporating certain simplifying assumptions has been written in order to enable rapid parametric analysis of many different Brayton cycle configurations. While the simplifying assumptions introduced result in small errors in the absolute values of the cycle efficiencies calculated, the relative values are sufficiently accurate to establish trends, determine sensitivity to various parameters, and evaluate the relative performance of the various system configurations.

* N. Y. Kirov, "Specific Heats and Total Heat Contents of Coals and Related Materials at Elevated Temperatures," The British Coal Utilization Research Association, Monthly Bulletin, Vol. XXIX, 33, 1965.

Efficiency values for a simple cycle, regenerative cycle, and regenerative cycle with one stage of intercooling are shown in Table VI. These data show that a regenerative cycle, as compared to a simple cycle, yields significantly higher efficiencies, and that peak efficiencies occur at lower compression ratios. A single stage of intercooling, coupled with regeneration, increases the cycle efficiencies of the order of 2 to 3 additional percentage points. Adding reheat and/or additional intercooling stages does not yield any further significant increases in cycle efficiency.

TABLE VI.

BRAYTON CYCLE EFFICIENCIES FOR VARIOUS SYSTEM CONFIGURATIONS, FUEL INLET CONDITIONS, TURBINE INLET TEMPERATURES AND COMPRESSION RATIOS

Cycle Configuration	Fuel Inlet Condition	Turbine Inlet Temp (°F)	Cycle Efficiency (%)						
			CR=4	CR=8	CR=12	CR=16	CR=20	CR=24	CR=30
Simple	P=1 ATM T=100°F	2000	19.8	27.3	30.6	32.4	33.4	33.9	34.2
		2500	20.3	28.4	32.1	34.3	35.8	36.8	37.8
		3000	20.6	29.0	33.0	35.4	37.1	38.3	39.6
	P=CR T=100°F	2000	21.8	29.4	32.6	34.2	35.0	35.5	35.7
		2500	22.3	30.4	33.9	35.9	37.1	38.0	38.7
		3000	22.7	31.0	34.7	36.9	38.3	39.3	40.2
	P=CR T=500°F	2000	24.0	32.4	35.9	37.8	38.9	39.4	39.7
		2500	24.6	33.5	37.4	39.7	41.1	42.1	43.0
		3000	24.9	34.1	38.2	40.7	42.3	43.4	44.6
Regenerative	P=1 ATM T=100°F	2000	41.5	40.0	37.1	34.3	31.8	29.4	26.3
		2500	45.2	45.3	43.5	41.6	39.8	38.0	35.7
		3000	47.7	49.0	47.9	46.6	45.2	43.9	42.0
	P=CR T=100°F	2000	44.2	43.8	41.6	39.3	37.2	35.3	32.6
		2500	47.9	49.2	48.0	46.5	45.1	43.7	41.8
		3000	50.4	52.8	52.3	51.4	50.4	49.4	48.0
	P=CR T=500°F	2000	45.5	45.4	43.4	41.3	39.3	37.4	34.8
		2500	49.2	50.8	49.8	48.5	47.2	45.9	44.2
		3000	51.7	54.5	54.2	53.5	52.6	51.7	50.5
Regenerative Plus Intercooler	P=1 ATM T=100°F	2000	43.0	43.7	42.6	41.4	40.2	39.2	37.7
		2500	46.3	48.2	47.8	47.1	46.4	45.6	44.6
		3000	48.6	51.3	51.4	51.1	50.6	50.1	49.3
	P=CR T=100°F	2000	45.8	47.5	47.0	46.1	45.3	44.5	43.3
		2500	49.1	52.0	52.2	51.8	51.4	50.9	50.1
		3000	51.4	55.1	55.8	55.8	55.6	55.3	54.8
	P=CR T=500°F	2000	47.0	49.0	48.6	47.9	47.2	46.4	45.4
		2500	50.3	53.6	53.9	53.7	53.3	52.9	52.3
		3000	52.7	56.7	57.5	57.7	57.6	57.4	57.0

Calculations were carried out to determine the sensitivity of gas turbine performance to variations in composition/heating value of the fuel gas. Table VII shows the effect on combustion temperature, turbine output, and cycle efficiency of varying the heating value of the fuel gas, assuming all other system

parameters, i.e., pressures, temperatures, flow rates, etc., remain fixed. These values indicate that a ±20% variation in fuel heating value will result in roughly a ±250°F variation in combustion temperature, and roughly a ±2 to 3% variation in cycle efficiency, provided no compensating adjustments are made. These numbers are large enough to be of concern. A 3% change in efficiency represents a significant change for a system being used for base load power generation. Also, a 250°F increase in turbine inlet temperature could significantly affect turbine blade life. The average heating value of the gas generated in Phase 1 of the Hanna II experiment is approximately 20% higher than that generated during the Hanna I experiment. During the Hanna I experiment, mean fuel heating values over successive two week intervals varied between -48% and +31% from the average over a 5-1/2 month period.* Furthermore, the mean value of the ratio of gas produced to air injected for successive two-week intervals varied between -17% and +9% from its average over the same period. In view of the above, it appears that some technique to compensate for expected fluctuations in fuel composition/heating value and production rate will be required.

TABLE VII

EFFECT OF FUEL HEATING VALUE (H) ON COMBUSTION TEMPERATURE (T), NET TURBINE OUTPUT (W), AND CYCLE EFFICIENCY (η) FOR A SIMPLE BRAYTON CYCLE WITH PRESSURE RATIO = 16 AND FUEL SUPPLIED @ 100°F & 1 ATM

H (BTU/SCF)	ΔH (%)	T (°R)	ΔT (%)	ΔW (%)	Δη Percentage	(%)
101	-20	2212	-10.1	-10.1	-2.9	-9.0
113	-10	2336	-5.0	-5.0	-1.3	-4.0
126	0	2460	0	0	0	0
139	+10	2585	+5.1	+5.1	+1.2	+3.7
151	+20	2709	+10.1	+10.1	+2.1	+6.5

One potential technique for averaging out, at least to some extent, undesirable fluctuations in gas composition, heating value, and production rate would be to manifold the output from multiple gas generators before routing the fuel to the turbine. A simple calculation, assuming the output of individual gas generators to be uniformly distributed with 3σ limits of ±50% of the mean, indicates that a minimum of 25 generators must be manifolded in order to reduce the 3σ limits on the output of the manifold to within ±10% of the mean. Another technique for compensating for fuel gas fluctuations would be to utilize a feedback control system which would monitor certain system parameter(s) (e.g., turbine inlet temperature, fuel composition, etc.) and use this information to regulate system flow

* L. A. Schrider and James W. Jennings, "An Underground Coal Gasification Experiment, Hanna, Wyoming," SPE Paper 4993 presented at the 49th Annual Fall Meeting of the Society of Petroleum Engineers, Houston, TX, October 6-9, 1974.

rates. Additional study is required to determine the details of how such a feedback control system should function.

2. Rankine Cycle Analysis:

Efficiency calculations were carried out for a conventional Rankine steam cycle with multiple feedwater heaters for both "hot" and "cold" fuel gas cleanup. A block diagram of a system employing two feedwater heaters is shown in Figure 17. Results of the efficiency calculations are shown in Table VIII for systems employing 0, 2, and 4 feedwater heaters. Actually, large commercial base load power plants often use as many as 6 or 8 feedwater heaters. However, the trend of the efficiency values with increasing number of feedwater heaters in Table VIII indicates that cycle efficiency could not be increased more than about one additional percentage point through use of additional feedwater heaters. Note that the Rankine cycle efficiencies are relatively independent of "hot" or "cold" fuel gas cleanup. Note also, as indicated in Figure 17, that the power conversion system, as was done in the case of the Brayton cycle, is supplying the power required to compress the injection air for the gasification process. If this power were charged to the gasification process rather than the power conversion system, each of the efficiency values in Table VIII would be increased by 2.6 percentage points.

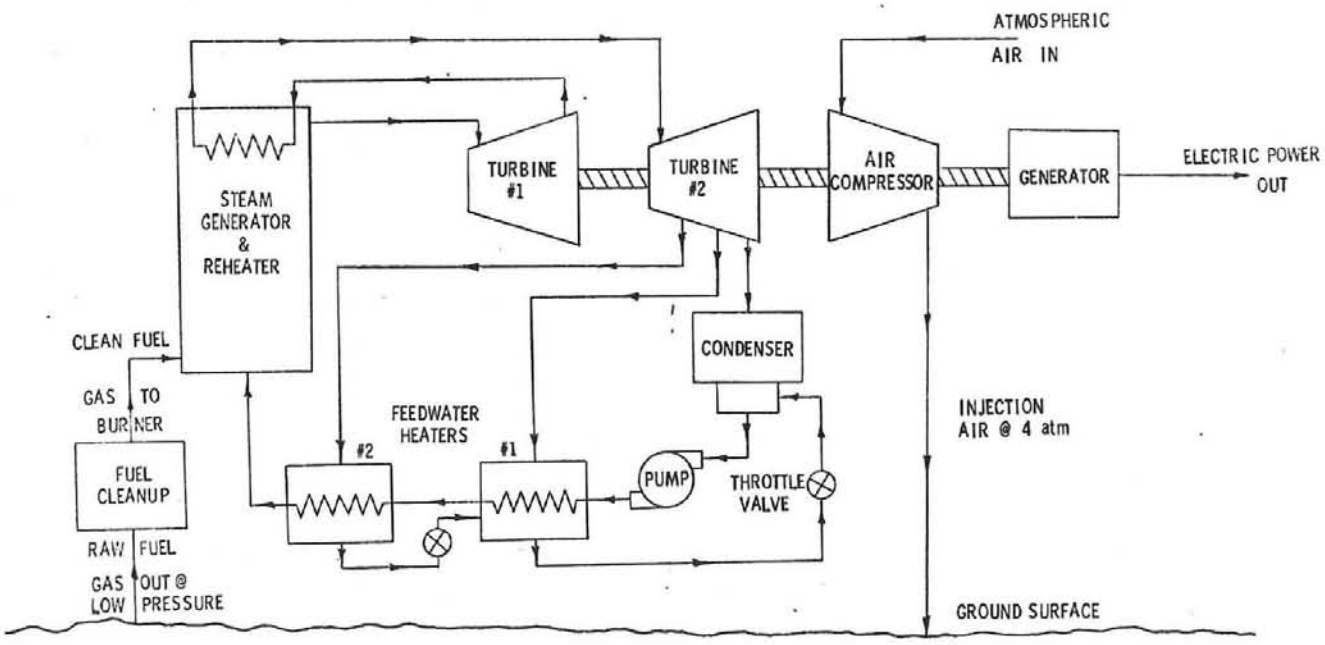

Figure 17. Rankine Power Cycle System with Two Feedwater Heaters.

TABLE VIII

RANKINE CYCLE EFFICIENCIES FOR SYSTEM UTILIZING MULTIPLE FEEDWATER HEATERS AND EITHER "HOT" OR "COLD" FUEL GAS CLEANUP

No. of Feedwater Heaters	Rankine Cycle Efficiency (%)	
	"Cold" Fuel	"Hot" Fuel
0	33.9	34.1
2	35.8	36.0
4	37.1	37.3

Calculation of combined cycle efficiencies for various cycle configurations and conditions are nearing completion. Preliminary indicates are that peak combined-cycle efficiencies will be only slightly higher than those for a Brayton cycle utilizing regeneration and intercooling. The relative economics of the two systems will be examined to determine whether the increase in efficiency justifies the added cost of a combined cycle.

VIII. PUBLICATIONS, PRESENTATIONS, AND BRIEFINGS

A. Publications

1. S. D. Stearns, "Attenuation of Acoustic Compressional Waves in Coal and Shale at Hanna, Wyoming," Sandia Laboratories Report, SAND-75-0471, November 1975.

2. H. M. Stoller, "In Situ Instrumentation Applied to Underground Coal Gasification," Sandia Laboratories Report, SAND-75-0459, September 1975.

3. D. A. Northrop, Editor, "Instrumentation and Process Control Development for In Situ Coal Gasification: Third Quarterly Report - June through August 1975," Sandia Laboratories Report, SAND-75-0535, October 1975.

B. Presentations

1. C. F. Brandenburg (LERC), R. P. Reed (Sandia), R. M. Boyd (LERC), D. A. Northrop (Sandia), and J. W. Jennings (U. of Wyoming, LERC), "Interpretation of Chemical and Physical Measurements from an In Situ Coal Gasification Experiment," presented by C. F. Brandenburg at the 50th Annual Fall Meeting of the Society of Petroleum Engineers of AIME, September 28 - October 1, 1975, Dallas, TX. Presentation published as Paper Number SPE 5654.

2. R. P. Reed, "Diagnostic Measurements for Field Research on In Situ Energy Conversion," presented at the Winter Meeting of the American Nuclear Society, San Francisco, CA, November 16-21, 1975. Extended abstract published in the Transactions of the American Nuclear Society 22, 5, 1975.

C. Briefings

1. Sandia Laboratories participated in a series of working group meetings held on various aspects of in situ coal gasification. These meetings, location, dates, and Sandia attendees are summarized below:

a. Instrumentation, Sandia, Albuquerque, NM, September 23, D. A. Northrop (Chairman), L. W. Beckham, and R. P. Reed.

b. Modeling, LLL, Livermore, CA, September 25, A. B. Donaldson.

c. Geology and Site Selection, LERC, Laramie, WY, October 8, D. A. Northrop and G. B. Griswold.

d. Field Operations, LERC, Laramie, WY, October 9, D. A. Northrop.

e. Environment and Health, ERDA, Washington, DC, October 15, S. G. Beard and M. L. Lieberman.

f. Laboratory Experimentation, MERC, Morgantown, WV, October 16, S. G. Beard and M. L. Lieberman.

2. D. A. Northrop, program briefing for G. A. Fowler, Vice President, and C. D. Broyles, Director of Field Engineering, Sandia Laboratories, at Hanna, Wyoming, November 19, 1975.

Distribution:

Mr. H. R. Johnson, Director
Office of Program Planning and Analysis
20 Mass. Ave., N.W.
Washington, D. C. 20545

Mr. J. W. Watkins
Acting Director
Oil, Gas and Shale Technology
U.S. ERDA/Fossil Energy
20 Mass. Ave., N.W.
Washington, D. C. 20545

Dr. H. N. Dunning
Acting Deputy Director
Oil, Gas and Shale Technology
U.S. ERDA/Fossil Energy
20 Mass. Ave., N.W.
Washington, D. C. 20545

Dr. G. A. Mills
Advanced Research and Supporting Technology
U.S. ERDA/Fossil Energy
20 Mass. Ave., N.W.
Washington, D. C. 20545

Dr. R. L. Zahradnik
Division of Coal Conversion and Utilization
U.S. ERDA/Fossil Energy
20 Mass. Ave., N.W.
Washington, D. C. 20545

Dr. J. D. Ham
Oil, Gas and Shale Technology
U.S. ERDA/Fossil Energy
20 Mass. Ave., N.W.
Washington, D. C. 20545

Mr. L. M. Burman
Oil, Gas and Shale Technology
U.S. ERDA/Fossil Energy
20 Mass. Ave., N.W.
Washington, D. C. 20545

Dr. P. R. Wieber
Oil, Gas and Shale Technology
U.S. ERDA/Fossil Energy
20 Mass. Ave., N.W.
Washington, D. C. 20545

Dr. J. Ramsey
Oil, Gas and Shale Technology
U.S. ERDA/Fossil Energy
20 Mass. Ave., N.W.
Washington, D. C. 20545

D. K. Nowlin, Director
Special Programs Division
U. S. ERDA
Albuquerque, New Mexico 87115
Attn: O. W. Wehlander

Ms. N. S. Hagen
San Francisco Operations Office
U. S. ERDA
1333 Broadway
Oakland, California 94616

A. W. Decora
L. A. Schrider (5)
C. F. Brandenburg
R. M. Boyd
D. D. Fischer
G. G. Campbell
Laramie Energy Research Center
U. S. ERDA
Laramie, Wyoming 82070

A. A. Pitrolo
J. Pasini, III
L. Z. Shuck
Morgantown Energy Research Center
U. S. ERDA
Morgantown, West Virginia 26505

J. S. Ball
Bartlesville Energy Research Center
U. S. ERDA
Bartlesville, Oklahoma 74003

I. Wender
Research Director
Pittsburgh Energy Research Center
U. S. ERDA
Bruceton, PA

K. Street, L-13
A. Maimoni, L-503
D. R. Stephens, L-437
J. D. Salisbury, L-156
Lawrence Livermore Laboratory
Livermore, CA 94550

T. Falkie, Director
U. S. Bureau of Mines
U. S. Department of the Interior
Washington, D. C. 20240

P. Russell
Denver Mining Research Center
Bldg. 20
Denver Federal Center
Denver, Colorado 80225

R. Balzhiser
Electric Power Research Institute
3412 Hillview Avenue
Palo Alto, California 94304

Distribution:

1 M. Sparks
2 W. J. Howard
1000 G. A. Fowler
1100 C. D. Broyles
1110 J. D. Kennedy
Attn: C. R. Mehl, 1111
H. D. Garbin, 1111
S. D. Stearns, 1111
L. D. Tyler, 1111
J. W. Wistor, 1116
R. P. Reed, 1116
1120 G. E. Hansche
Attn: B. C. Benjamin, 1123
J. A. Beyeler, 1123
1130 H. E. Viney
Attn: R. D. Statler, 1133
W. C. Wilson, 1133
1300 D. B. Shuster
5000 A. Narath
5100 J. K. Galt
Attn: W. Herrmann, 5160
5200 E. H. Beckner
5400 A. W. Snyder
5700 J. H. Scott
5710 G. E. Brandvold
Attn: M. M. Newsom, 5718
5730 H. M. Stoller (5)
Attn: G. B. Griswold, 5731
M. L. Lieberman, 5731
J. C. Mitchell, 5731
B. L. Sewell, 5731
5732 D. A. Northrop (30)
Attn: S. G. Beard, 5732
L. W. Beckham, 5732
L. C. Bartel, 5732
5733 C. L. Schuster
Attn: R. G. Hay, 5733
L. J. Keck, 5733
R. P. McCann, 5733
R. W. Seavey, 5733
5740 V. L. Dugan
Attn: S. G. Varnado, 5742
R. E. D. Stewart, 5742
5800 R. S. Claassen
5820 R. L. Schwoebel
Attn: R. W. Lynch, 5824
A. W. Mullendore, 5825
5840 D. M. Schuster
Attn: R. C. Heckman, 5842
H. P. Stephens, 5842
R. U. Acton, 5842
8000 T. B. Cook, Jr.
8110 A. N. Blackwell
Attn: D. Hartley, 8115
9350 F. W. Neilson
Attn: O. J. Burchett, 9352
J. C. Bushnell, 9352
J. H. Gieske, 9352
9420 T. L. Pace
Attn: J. L. Rodgers, 9422
R. J. Bayette, 9422
G. L. West, 9423
T. M. Schultheis, 9423
F. D. Gutierrez, 9424
W. D. Swartz, 9424
8266 E. A. Aas (2)
3141 L. S. Ostrander (5)
3151 W. L. Garner (3)
for ERDA/TIC (25)
Attn: R. P. Campbell, 3171-1